Journal of Hydrology 653 (2025) 132765

Contents lists available at ScienceDirect

Journal of Hydrology

journal homepage: www.elsevier.com/locate/jhydrol

Research papers

Dynamic and high methane emission flux in pond and lake aquaculture

Jiayu Zhao [a], Mi Zhang [b,c], Yini Pu [d], Lei Jia [b], Wei Xiao [b,c], Zhen Zhang [e], Pei Ge [b], Jie Shi [b], Qitao Xiao [f], Xuhui Lee [g]

[a] College of Ocean and Meteorology/South China Sea Institute of Marine Meteorology (SIMM), Guangdong Ocean University, Zhanjiang 524088 China
[b] Yale-NUIST Center on Atmospheric Environment, Nanjing University of Information Science and Technology, Nanjing 210044 China
[c] Key Laboratory of Ecosystem Carbon Source and Sink, China Meteorological Administration (ECSS-CMA), Nanjing University of Information Science and Technology, Nanjing 210044 China
[d] Office of Development Planning and Discipline Construction, Chengdu University of Technology, Chengdu 610059 China
[e] Nanjing Jiangning District Meteorological Bureau, Nanjing 211100 China
[f] Key Laboratory of Watershed Geographic Sciences, Nanjing Institute of Geography and Limnology, Chinese Academy of Sciences, Nanjing 210008 China
[g] School of the Environment, Yale University, New Haven 06511 USA

ARTICLE INFO

This manuscript was handled by Huaming Guo, Editor-in-Chief, with the assistance of Mahmood Sadat-Noori, Associate Editor

Keywords:
Aquaculture ponds
Lake aquaculture
High-resolution in-situ measurements
Methane flux
Temperature sensitivity

ABSTRACT

Freshwater aquaculture systems are recognized as significant contributors to atmospheric methane (CH_4) emissions, yet accurate quantification remains challenging due to high variability across different aquaculture types and the scarcity of high-frequency observations. To address these gaps, we conducted synchronous in-situ measurements of CH_4 emissions from two typical aquaculture types – pond aquaculture and lake aquaculture – in the Yangtze River Delta, China, using the eddy covariance technique, capturing CH_4 flux from hourly to annual scales. Our high-resolution measurements revealed a weak diurnal pattern in CH_4 flux, although daily mean flux varied considerately at the two systems (lake aquaculture: 0.04 to 6.60 μg CH_4 m^{-2} s^{-1}; pond aquaculture: 0.08 to 15.4 μg CH_4 m^{-2} s^{-1}). CH_4 flux was significantly higher in the pond aquaculture compared to the lake aquaculture, with the annual mean value of 5.08 μg CH_4 m^{-2} s^{-1} (120 g CH_4-C m^{-2} yr^{-1}) and 1.52 μg CH_4 m^{-2} s^{-1} (36 g CH_4-C m^{-2} yr^{-1}), respectively. Further analysis suggested that smaller size of the ponds, combined with higher nitrogen and carbon loadings and elevated chlorophyll-a concentrations, likely contributed to substantial emissions from the pond aquaculture. Ebullition was identified as the primary emission pathway, accounting for 70 % and 60 % of the total CH_4 emissions from the pond and the lake system, respectively. While CH_4 flux increased significantly with increasing temperature, the flux during the warming phase of the year was lower than during the cooling phase at equivalent temperatures. Additionally, CH_4 flux in the pond system was less sensitive to temperature than in the lake system (Q_{10} for pond: 2.29; Q_{10} for lake: 5.75), likely due to the compound influence of biotic factors. Our findings underscore the importance of incorporating high-resolution emissions data from diverse aquaculture systems to accurately estimate the CH_4 budget of freshwater aquaculture.

1. Introduction

The renewed rapid growth of atmospheric methane (CH_4) (10.2 ppb/year) has motivated research on freshwater ecosystems, which are regarded as the largest natural source of CH_4 (Rosentreter et al., 2021; Rocher-Ros et al., 2023; Thanwerdas et al., 2024). Among freshwater natural ecosystems like boreal wetlands and tropical rivers are significant CH_4 sources (Borges et al., 2015, 2022; Saunois et al., 2024), these human-impacted ecosystems have received considerable attention because their CH_4 emissions are sensitive to human activities (Xiao et al., 2017; Beaulieu et al., 2019; Rocher-Ros et al., 2023). Significant CH_4 emissions rates have been reported for freshwater aquaculture due to intense management practices (Yuan et al., 2019; Kosten et al., 2020). The total CH_4 emission from the global freshwater aquaculture systems is estimated to be 6 to 14 Tg CH_4 yr^{-1} (Yuan et al., 2019; Rosentreter et al., 2021). Importantly, it is projected that aquaculture production worldwide will expand rapidly to keep pace with the escalating demand for protein sources (FAO, 2022; Zhang et al., 2022b), which will further amplify the role in aquacultural CH_4 emission in the global CH_4 cycle (Yuan et al., 2019; Gephart et al., 2021; Naylor et al., 2021; Dong et al., 2022). Thus, accurate quantification of CH_4 emissions from aquaculture ecosystems is necessary for mitigating CH_4 emissions from human-

E-mail addresses: zhangm.80@nuist.edu.cn (M. Zhang), qtxiao@niglas.ac.cn (Q. Xiao), xuhui.lee@yale.edu (X. Lee).

https://doi.org/10.1016/j.jhydrol.2025.132765
Received 30 October 2024; Received in revised form 4 January 2025; Accepted 17 January 2025
Available online 1 February 2025

dominated freshwater systems (Tong et al., 2021; Chen et al., 2023; Saunois et al., 2024; Yang et al., 2024a, b).

One major reason for the large uncertainty is that aquaculture CH_4 emission varies significantly among different aquaculture types. Pond aquaculture and lake aquaculture, the two predominant types of freshwater aquaculture, exhibit distinct emission dynamics and intensities. However, the IPCC only uses a single emission factor (EF: 183 kg CH_4 ha^{-1} yr^{-1}) to obtain the global freshwater aquaculture emission estimate (IPCC, 2021); This estimate is likely biased due to the lack of integration across diverse aquaculture types (Yuan et al., 2019; Dong et al., 2022). In theory, lake aquaculture, characterized by its larger size and natural water exchange, should emit less CH_4 per unit surface area due to the dilution of organic matter (Holgerson and Raymond, 2016). Other factors, such as low primary production rate and stable thermal stratification in large lake systems may also contribute to low CH_4 emissions (Borges et al., 2022). However, aeration and dredging, two common management practices in pond aquaculture, can substantially decrease CH_4 emission (Yang et al., 2018, 2019; Fang et al., 2022; Nijman et al., 2022). Since these practices are not used in lake aquaculture, possibility exists that some pond systems may emit less CH_4 than lake aquaculture in the same climate. Currently, there is a focus on pond-based CH_4 emissions (Tong et al., 2021; Yang et al., 2019, 2024b; Yuan et al., 2021; Zhao et al., 2021), yet there is a scarcity of CH_4 emission observations in lake aquaculture (Pu et al., 2022). This imbalance in research likely skews our understanding of CH_4 emission processes in freshwater aquaculture.

Large temporal variabilities in CH_4 flux are another factor that contributes to the uncertainty in the CH_4 emission estimates. Methane emission from aquaculture systems is influenced by complex biogeochemical processes and is shaped by biotic factors (e.g., nutrients loading) and abiotic factors (e.g., temperature). These factors vary across a spectrum of time scales, leading to short-term (hourly) fluctuations in CH_4 flux and long-term trends that span seasons and years (Podgrajsek et al., 2014; Natchimuthu et al., 2016; Sieczko et al., 2020; Zhang et al., 2022c; Yang et al., 2024). Despite considerable temporal fluctuations in the flux, most studies have relied on snapshot samplings and daytime-only measurements at a low sampling frequency (monthly or seasonal) to obtain annual total emission rates (Kosten et al., 2020; Zhang et al., 2023b). The lack of temporal resolution may represent a large source of uncertainties (Wik et al., 2016; Duan et al., 2023). CH_4 flux from natural freshwater ecosystems often exhibit substantial diurnal fluctuations, with differences between different times of day exceeding 200 % (Xiao et al., 2014a; Zhang et al., 2019a; Hu et al., 2020; Tan et al., 2021). But the diel variation of aquacultural CH_4 flux is poorly understand due to the lack of continuous and high-frequency measurements (Kosten et al., 2020).

China is a hotspot region of CH_4 emissions from aquaculture. It is the world's largest freshwater aquaculture producer, contributing over 60 % of global aquaculture production and 58 % of CH_4 emissions from freshwater aquaculture systems among the top 21 global producers (Yuan et al., 2019; FAO, 2022). With the increasing need for protein diet, China's freshwater aquaculture is projected to further increase in both production and area in the coming decades (Cao et al., 2015; FAO, 2022). The Yangtze River Delta (YRD) in eastern China is an important region for freshwater aquaculture, accounting for 26 % of the country's total aquaculture area (China Fishery Statistical Yearbook, 2023). Because both pond and lake aquaculture are practiced, the YRD region offers an opportunity to compare and contrast emission rates and patterns between these two systems under the same climate conditions. Although previous studies have compared aquacultural CH_4 emission across different types in China (Yuan et al., 2019; Zhang et al., 2022d; Dong et al., 2022), they have been based on *meta*-analysis of data collected over different climate zones and without consideration of temporal variations. Furthermore, continuous measurements have been rare. In recent years, aquaculture in China has gradually shifted from lake to pond systems, driven by ecological restoration policies. This shift caused an 18 % reduction in lake and reservoir aquaculture area and a 10 % increase in pond aquaculture from 2016 to 2022 (China Fishery Statistical Yearbook, 2023). Synchronized observations in both systems are needed to determine whether this policy-driven shift has resulted in an overall reduction in CH_4 emission.

In this study, we employed the eddy covariance (EC) technique to simultaneously measure CH_4 flux at an aquaculture pond complex and at an aquacultural lake in the YRD. The EC technique, which provides in-situ measurement of the flux at half-hourly to hourly timesteps, have been employed in studies of natural lake and reservoir systems (e.g., Eugster et al., 2011; Podgrajsek et al., 2014; Zhang et al., 2019; Waldo et al., 2021; Hounshell et al., 2023). However, the application of this technique in aquaculture systems is still limited. There are two motivations for this study. Firstly, we are interested in temperature-dependent behaviors of the flux. Previous studies have suggested that the flux sensitivity to temperature may vary across different aquaculture types (Davidson et al., 2015; Zhu et al., 2020). Measurements at high temporal resolutions should help resolve this issue, therefore allowing more robust projection of how aquaculture CH_4 emission may respond to future climate warming. Secondly, ebullition, an important CH_4 emission pathway, is size dependent (Bastviken et al., 2004; Yang et al., 2020). Even though the eddy covariance technique measures the total CH_4 flux, it is now possible to isolate the ebullition component using high frequency (e.g. 10 Hz) data collected by eddy covariance (Iwata et al. 2018). Because aquaculture ponds are much smaller than aquaculture lakes, eddy covariance collected in these two systems provides a good opportunity to further investigate the size-dependence of the ebullition contribution to the total CH_4 flux. Specifically, the objectives of this study are: (1) to compare temporal patterns of CH_4 flux between the two aquacultural systems; (2) to quantify their annual CH_4 emission and the ebullition contribution; and (3) to investigate biotic and abiotic factors that regulate the CH_4 flux across multiple time scales.

2. Materials and methods

2.1. Sites

The aquaculture pond and the aquaculture lake were both situated in the YRD, Eastern China, a region characterized by a subtropical humid monsoon climate (Fig. 1a). The mean air temperature and annual rainfall were 18.0 °C and 1290 mm at the lake site, and 17.5 °C and 1330 mm at the pond site in 2018. The pond site was in the middle of four fishponds (31° 58′ N, 118° 15′ E), each having a mean water depth of 1.8 m and an area of about 0.7 ha (Fig. 1b). The lake site was situated in the southeast corner of Lake Taihu (31° 03′N, 120° 28′ E, Fig. 1c), with a mean water depth of 1.3 m, in an extensive aquaculture area of about 10600 ha in size (Qin et al., 2007; Pu et al., 2022). Both aquaculture systems were established in the 1980 s and have never been dredged.

Both aquaculture systems utilized a polyculture practice prevalent in the YRD region. At the pond, the polyculture system was dominated by six fish species mixing with clams. They received a commercial diet three times daily. To promote phytoplankton growth, chicken manure was applied twice per year, once in early February and again in late November. The lake aquaculture primarily stocked Chinese mitten crab, and was supplemented with black shrimp and giant river prawn. The annual feed input were 8570 kg C/ha and 6400 kg C/ha at the pond and the lake system, respectively.

2.2. CH_4 flux and supporting measurements

The EC observation took place at the two sites using two identical EC systems. Each EC system consisted of an open-path CO_2/H_2O infrared gas analyzer (Model EC150, Campbell Scientific Inc., Logan, Utah, USA), a three-dimensional sonic anemometer/thermometer (Model CSAT3A, Campbell Scientific Inc.), and an open-path CH_4 analyzer (Model LI-7700, LI-COR Inc., Lincoln, Nebraska, USA). They measured the fluxes

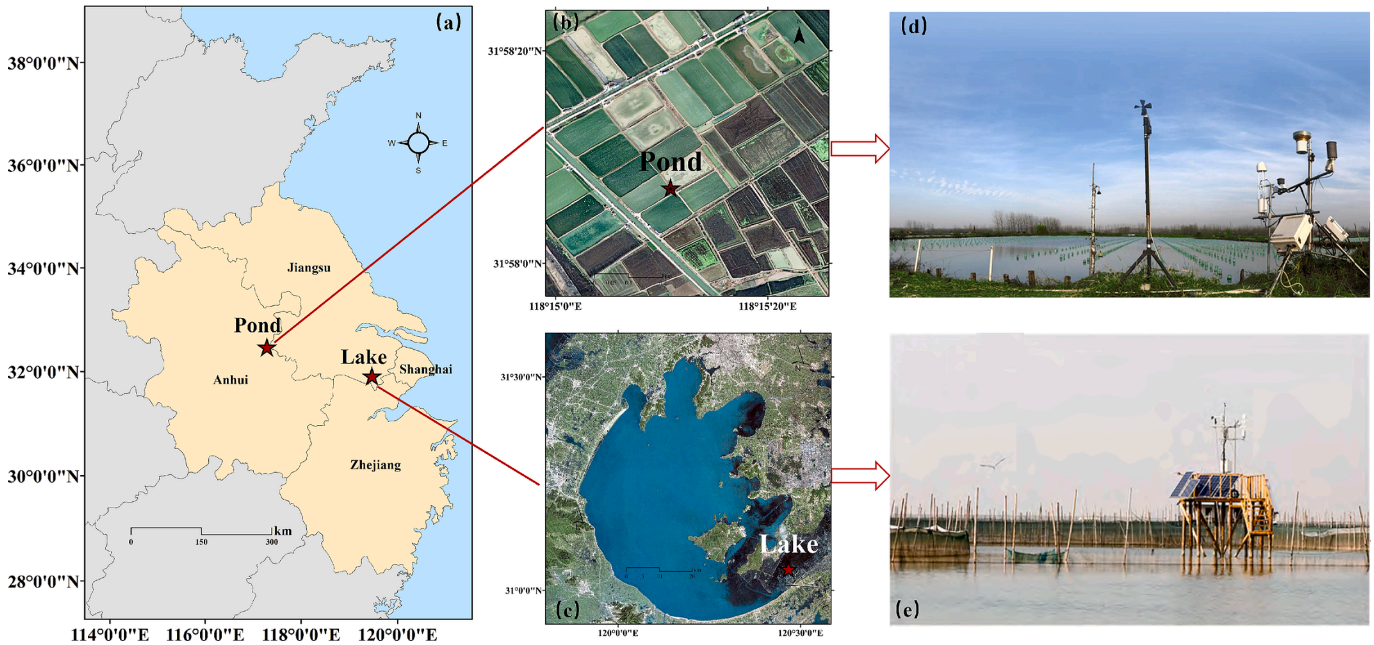

Fig. 1. (a) Map showing site locations in the Yangtze River Delta; (b) and (c) satellite images of the fish ponds and Lake Taihu; (d) and (e) photographs of the instrument setup and the measurement platform. Stars in b and c mark measurement locations.

of momentum, sensible heat, latent heat or water vapor, CO_2 and CH_4. The observation height was approximately 1.0 m and 5.0 m above the water surface at the pond and the lake, respectively. Raw data were collected using a data logger (Model CR3000, Campbell Scientific Inc.) at a sampling frequency of 10 Hz. The results presented in this study span the period from January to December 2018 at the pond and from March to December 2018 at the lake.

Ancillary meteorological data were collected at the sites. Air temperature and air humidity were measured using a temperature/humidity probe (Model HMP155, Vaisala Inc., Helsinki, Finland). Wind speed and direction were observed using the three-dimensional sonic anemometer and a wind vane (Model 05103, R M Young Company, Traverse City, Michigan, USA). The four components of the surface net radiation were monitored with a four-way net radiometer (Model CNR4, Kipp&Zone B. V., Delft, the Netherlands). Water temperature at 20 cm below the water surface and sediment temperature at the depth of 5 cm were observed using temperature probes (Model 109-L, Campbell Scientific Inc.). All parameters were recorded at 1 Hz and archived as half-hourly averages by a datalogger.

In addition to micrometeorological variables, water chemical properties were measured at several locations. At the pond site, pH and dissolved oxygen concentration (DO) were observed at the 20 cm depth using a multi-parameter probe (Model: YSI 650MDS, YSI Inc., Yellow Springs, Ohio, USA), typically once per season. Water samples were collected at the same locations and the same time for analysis of dissolved organic carbon (DOC), total phosphorus (TP) and total nitrogen (TN), NO^-_3-N, NH^+_4-N, Chl-a concentration. At the lake, surface water samples were collected at a depth of 50 cm during each season: winter in February, spring in May, summer in August, and autumn in November. These samples were stored on ice while in the field and then transported to the Taihu Laboratory for Lake Ecosystem Research for analysis of water quality parameters (Zhang et al., 2016; Xiao et al., 2024).

2.3. Data processing and gap filling

The standard procedure embedded in the EddyPro software (version 6.2.1; LI-COR Inc.) was used to process the 10 Hz EC data to derive half-hourly fluxes. A number of processing steps were implemented in EddyPro. A series of quality control criteria were applied to screen raw data for spikes (Vickers and Mahrt, 1997). Time lags resulting from spatial separations between the analyzers and the sonic anemometer were compensated using a cross-covariance maximization method (Horst and Lenschow, 2009). A double coordinate rotation was executed to force the mean vertical wind velocity to zero for each 30-min period (Lee et al., 2004). The WPL correction was applied to eliminate the effect of density fluctuations arising from variations in water vapor and temperature (Webb et al., 1980). The spectroscopic effect caused by temperature, pressure, and water vapor fluctuations on the shape of the CH_4 absorption line was rectified using the method outlined by McDermitt et al. (2011). High-frequency damping losses were assessed and corrected using the method proposed by Moncrieff et al. (1997). The 0–1-2 quality flag system developed by Mauder and Foken (2004) was utilized to classify flux data. Each 30-min datapoint was given a quality flag, categorized as 0 (best quality), 1 (good quality), or 2 (bad quality). Data with flags 0 and 1 were kept for further analysis. Flag 2 marks periods with the CH_4 relative signal strength indicator (RSSI) value below 10 %, instrument maintenance, or rain interference; these periods were excluded. Furthermore, a flux footprint analysis conducted at the pond sites revealed that about 80 % of the footprint fell within the targeted ponds, and the footprint peak was always located inside the pond boundary (Zhao et al., 2019; Zhao et al., 2021). Outside these ponds were also wet surfaces (rice paddies) whose CH_4 flux was similar in magnitude to the pond flux (Section 4.2). Of the three gases we measured (CH_4, CO_2 and H_2O), CH_4 flux was the least affected by the surface source heterogeneity (Zhao et al., 2019). Overall, 44 % and 43 % of the CH_4 flux observations passed these data quality control checks at the lake and the pond sites, respectively.

The daily flux was determined by averaging all valid half-hourly observations on days with the 30-min flux data above 40 %. The valid daily CH_4 flux represented 56 % and 31 % of the total observational periods at the lake and pond, respectively. We employed the random forest (RF) method to fill the gaps in the daily CH_4 flux. Monthly and annual fluxes were determined with the gap-filled daily flux. As a supervised machine learning algorithm, RF is the optimal choice for completing the CH_4 flux dataset, especially for long gaps. This is because of its robustness against over-fitting, which is a key concern when using artificial neural networks, especially when dealing with limited training periods or noisy data (Kim et al., 2020; Mahabbati et al., 2021). All valid data were first divided into two subsets: a training set (70 %) and a validation set (30 %). The RF model was initially built based on the training dataset and then was used to predict the CH_4 flux of the validation set. The input data used as predictors include global radiation, sediment temperature, wind speed, atmospheric pressure, relative humidity, precipitation, and day of year. These variables were obtained from ancillary micrometeorology measurements. Overall, the agreement between the prediction and the observation is satisfactory, with a coefficient of determination (R^2) of 0.92 and 0.85 and a root mean square error (RMSE) of 0.44 μg CH_4 m^{-2} s^{-1} and 0.48 μg CH_4 m^{-2} s^{-1} for the lake and the pond, respectively.

2.4. Estimating CH_4 ebullition

A partitioning method developed by Iwata et al. (2018) was utilized to isolate the ebullitive flux from the total CH_4 flux measured with the EC instruments. This method has been successfully applied in various ecosystems, including lakes, rice paddies, and bogs (Hwang et al., 2020; Pu et al., 2022; Taoka et al., 2020; Ueyama et al., 2022). It relies on the local-scale similarity between the CH_4 concentration and other scalar components, like H_2O concentration and air temperature, in the wavelet domain. It assumes that the ebullitive flux can be characterized by dissimilar fluctuations between the CH_4 concentration and a reference scalar. In this study, air temperature was chosen as the reference scalar. Wavelet coefficients between the CH_4 concentration and air temperature were calculated using a wavelet transform. An iteratively re-weighted linear regression was applied between the converted wavelet coefficients of CH_4 concentration and air temperature at the same scale. If wavelet coefficients significantly deviated from the fitted regression line and were greater than three times the minimum of root mean squared deviation for each month, this signal was considered to be ebullitive.

2.5. Determining temperature sensitivity

The temperature sensitivity of CH_4 flux is commonly characterized by the Q_{10} factor, which quantifies the proportional change over a 10 °C increase in temperature. We employed the Q_{10} method described by DelSontro et al. (2016), focusing on the "ecosystem-level" Q_{10}. This approach accounts for the cumulative effects of multiple biotic and abiotic factors that influence CH_4 flux. The Q_{10} for CH_4 flux was estimated using the formula $Q_{10} = e^{10b}$, where b represents the slope of the linear relationship between temperature and the natural logarithm of the observed CH_4 flux. This calculation was applied to daily flux data.

2.6. Data analysis

Single-variable regression was conducted to investigate the relationships between CH_4 fluxes with environmental factors across different time scales. The best-fit regression equation for CH_4 flux and temperature, along with p value and adjusted linear correlation R, were presented. Student's t-test was used to determine the significant differences between the two aquaculture types, with a significance level set at $p < 0.05$. All data processing and statistical analysis were performed with the MATLAB software (MathWorks, Inc., Natick, MA, USA).

3. Results

3.1. Temporal variations in environmental conditions

Significant differences in water quality parameters were observed between the pond and the lake, with the pond exhibiting markedly higher levels across all metrics ($p < 0.05$, Fig. 2, Table S1). The annual mean concentrations of nutrient indicators, including TN, TP, $NH^{+}{}_{4}$-N, and $NO^{-}{}_{3}$-N at the pond exceeded those at the lake by two to four times, with the $NH^{+}{}_{4}$-N concentration showing the largest difference of 13 times (Fig. 2a–d, Table S1). This nutrient enrichment at the pond was caused by abundant feed, small waterbody size and stagnant conditions. The mean DOC and Chl-a concentration at the pond were significantly higher, by an average of five times more, than those at the lake (Fig. 2e–f).

Seasonally, the concentrations of TN, $NH^{+}{}_{4}$-N, and $NO^{-}{}_{3}$-N were generally lower in the summer and the autumn than the winter and the spring at the two sites, primarily attributed to the higher denitrification rate, rainfall dilution, and phytoplankton uptake (Xu et al., 2010). At the pond, the reductions were significant, with TN decreasing by 39 %, $NH^{+}{}_{4}$-N by 15 %, and $NO^{-}{}_{3}$-N by 71 %. At the lake, the reductions were less pronounced but still substantial: TN by 18 %, $NH^{+}{}_{4}$-N by 49 %, and $NO^{-}{}_{3}$-N by 65 %. Additionally, the DOC concentration at the pond showed a substantial reduction of 43 % in the summer and the autumn compared to the winter and the spring, whereas the seasonality was not as evident at the lake.

In contrast to water quality, there were no large differences in physical factors such as water temperature (T_w), sediment temperature (T_s), and net radiation (R_n) between the pond and the lake, except for

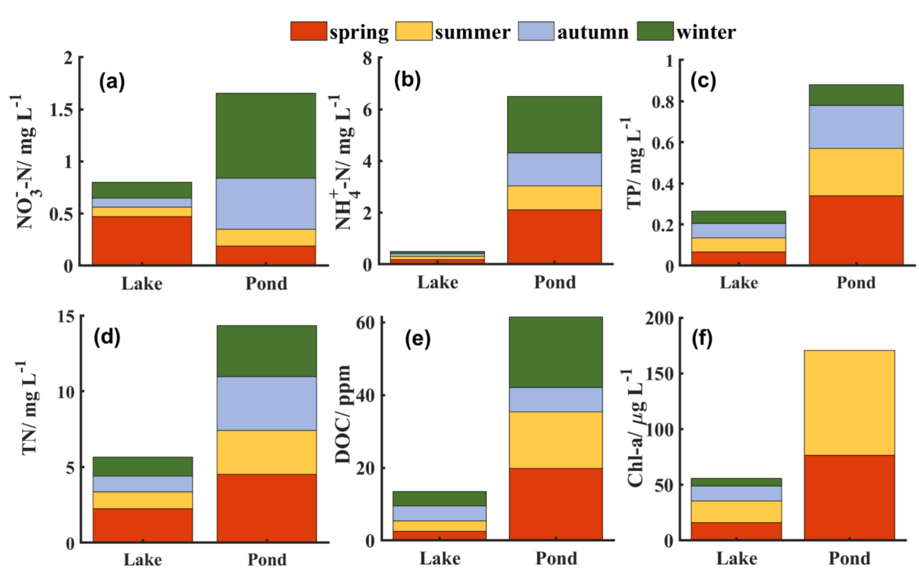

Fig. 2. Seasonal mean value of (a) $NO^{-}{}_{3}$-N concentration, (b) $NH^{+}{}_{4}$-N concentration, (c) total phosphorus (TP) concentration, (d) total nitrogen (TN) concentration, (e) dissolved organic concentration (DOC), and (f) Chlorophyll a (Chl-a) concentration in the water column at the lake and the pond site.

wind speed (Table S1). Both the pond and the lake exhibited similar and significant diurnal and seasonal patterns in these factors (Fig. 3). Specifically, both systems displayed diurnal and seasonal patterns in T_w and T_s, with generally higher values during the daytime than at night and during the summer than during the winter (Fig. 3, Table S1). The lake and pond sites showed similar annual mean values of T_w of 18.8 °C and 18.5 °C and T_s of 19.9 °C and 19.7 °C, respectively. The net radiation also followed a strong temporal pattern, reaching its peak during the month of July. The annual mean R_n values were comparable, at 105.7 W/m^2 and 103.2 W/m^{2}at the lake and the pond site, respectively. The wind speed showed different seasonal and diurnal patterns between the sites. Higher values were observed during the daytime than night and in the winter and the spring than in the summer and the autumn at the pond; these patterns were reversed at the lake (Table S1). The annual mean wind speed at the lake site (3.17 m/s) were significantly higher than that at the pond site (2.04 m/s), primarily due to the large open water fetch at the lake site.

3.2. Diurnal and seasonal CH_4 flux

The two systems show different diurnal pattern of CH_4 flux (Fig. 4, Table S2). In the lake system, the flux was higher at night (20:00 to 04:00 local time), by an average 9 %, than during the day (08:00 to 16:00 local time). The most pronounced diurnal difference occurred in the winter, with the nighttime flux exceeding the daytime flux by 29 %, followed by 17 % in the autumn and 7 % in the summer (Table S2). In contrast, the pond exhibited a slightly higher flux in the daytime, by an average of 4 %, than at night. The diurnal difference at the pond peaked at 13 % in the autumn, followed by 7 % in the winter, 2 % in the summer, and 1 % in the spring.

In terms of the CH_4 flux seasonality, both systems exhibited peak values in the summer (June to August; Fig. 5a & b and Table S2), with a seasonal mean of 3.35 μg CH_4 m^{-2} s^{-1} at the lake and 9.61 μg CH_4 m^{-2} s^{-1} at the pond. The summer season accounted for 56 % and 50 % of the annual total emission at the lake and the pond, respectively. The lowest flux was observed during winter months (January, February, and December), the seasonal mean value being 0.26 μg CH_4 m^{-2} s^{-1} at lake and 0.62 μg CH_4 m^{-2} s^{-1} at the pond. The daily CH_4 flux at the lake ranged from 0.04 μg CH_4 m^{-2} s^{-1} to 6.60 μg CH_4 m^{-2} s^{-1}, with an annual mean value of 1.52 μg CH_4 m^{-2} s^{-1}. At the pond, the variation range and the mean value were both greater, with the daily flux ranging from 0.08 μg CH_4 m^{-2} s^{-1} to 15.4 μg CH_4 m^{-2} s^{-1} and the annual mean of 5.08 μg CH_4 m^{-2} s^{-1}. Seasonally, the CH_4 flux at the pond was 6.0, 2.9, 3.4, and 2.4 times higher than at the lake in the spring, summer, autumn, and winter, respectively (Table S2). It is noted that the negative half-hourly flux in Fig. 5 was caused by random errors, which is also present in other eddy covariance studies (e.g., Eugster et al., 2011; Podgrajsek et al., 2014; Waldo et al., 2021).

The annual gap-filled flux at the pond (1200 kg CH_4-C/ha) was approximately three times higher than at the lake (360 kg CH_4-C/ha). This difference was largely due to the frequent high half-hourly flux episodes (> 5 μg CH_4 m^{-2} s^{-1}) observed at the pond. Approximately 38 % of half-hourly measurements surpassed 5 μg CH_4 m^{-2} s^{-1} at the pond, whereas only 8 % of the observations were above this threshold at the lake (Fig. 5c).

3.3. CH_4 ebullition

Over the annual period, ebullition was the major pathway for CH_4 emissions at both sites, contributing 60 % and 70 % (median value) or 60 % and 67 % (mean value) to the total CH_4 emission at the lake and pond, respectively (Fig. 6a). There was no significant difference of the ebullition ratio between the two systems across different seasons (Fig. 6a), but the ebullitive rate was different (Fig. 6b). The ebullitive rate demonstrated clear seasonal variation at both sites, with the highest ebullition flux observed between July and September. The monthly mean ebullition rate at the lake and the pond was in the range of 0.07 to 2.43 μg CH_4 m^{-2} s^{-1} and 0.24 to 9.04 μg CH_4 m^{-2} s^{-1}, respectively. The annual mean ebullition rate at the pond (4.33 μg CH_4 m^{-2} s^{-1}) was much higher than at the lake (1.17 μg CH_4 m^{-2} s^{-1}).

3.4. Factors influencing CH_4 flux

Among various meteorological factors, CH_4 flux at both sites showed a significant and positive correlation with temperatures at half-hourly, daily, and monthly scale (Table S3). At the daily scale, the relationship was exponential (Fig. 7a), with sediment temperature having the highest R value (lake: 0.82; pond: 0.80), followed by water temperature (lake: 0.77; pond:0.77) and air temperature (lake: 0.74; pond: 0.69). In other words, variations in sediment temperature explained over 60 % of

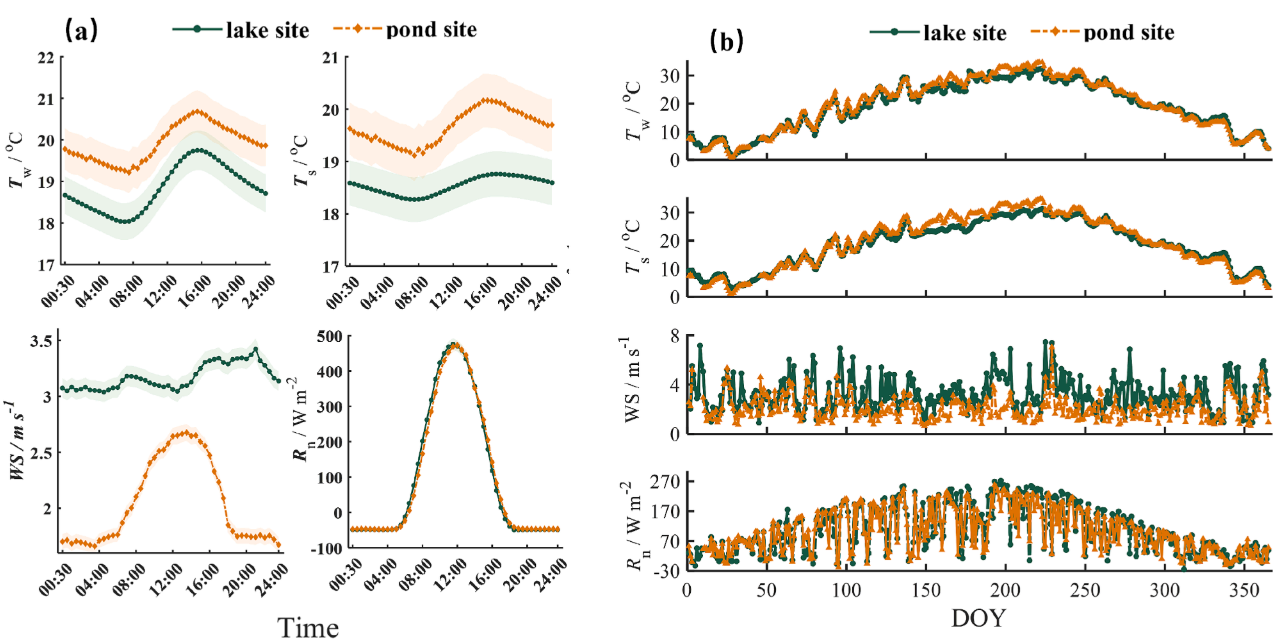

Fig. 3. (a) Diurnal and (b) daily variation of environmental variables: T_w: water temperature, T_w: sediment temperature, *WS*: wind speed, R_n: net radiation.

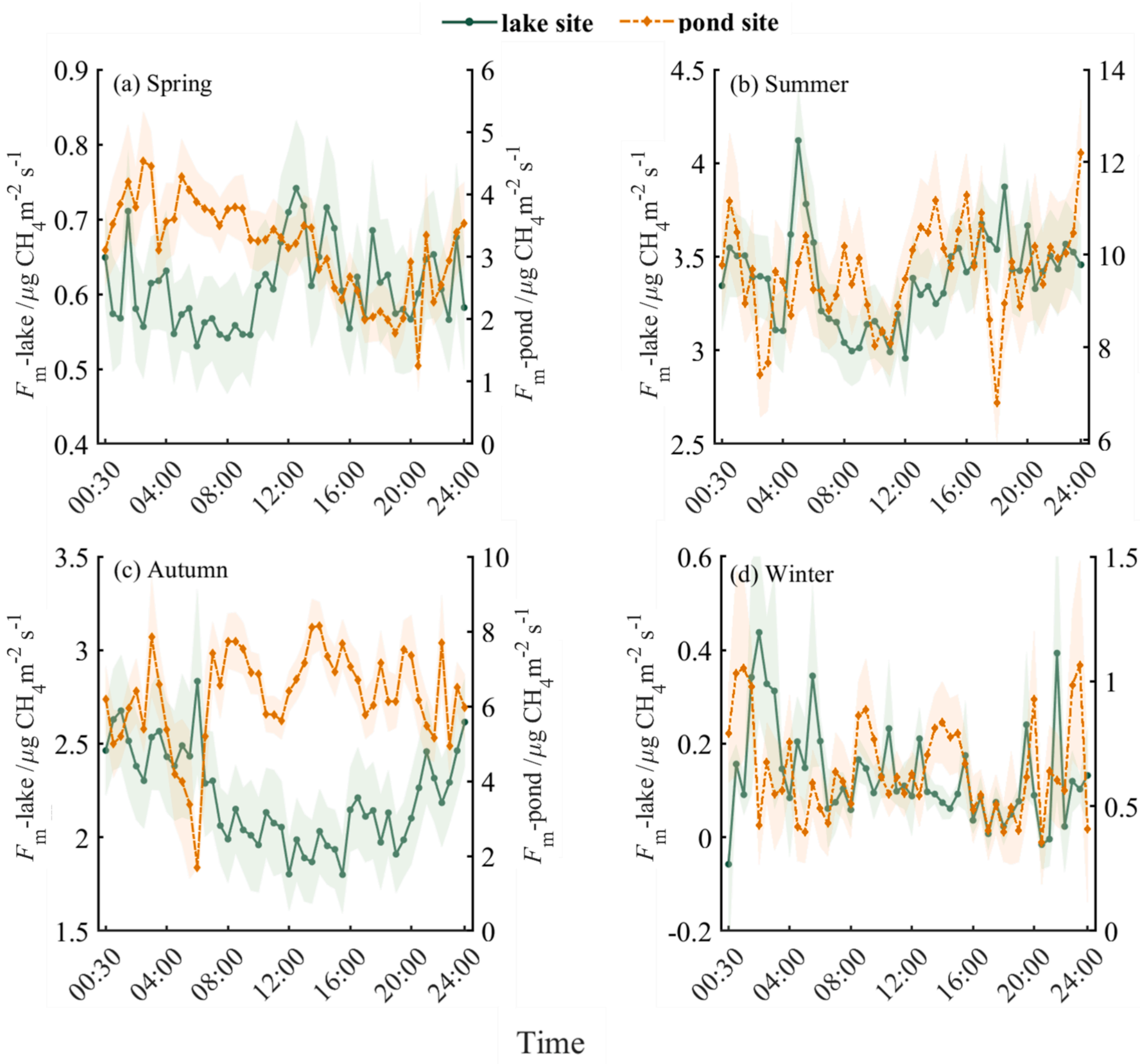

Fig. 4. Diurnal variation in half-hourly CH_4 flux (Mean ± Standard error) in four different seasons.

the flux variations. The CH_4 flux was more sensitive to temperature at the lake (Q_{10}: 5.75) than at the pond (Q_{10}: 2.29). Notably, there was a clear temperature hysteresis at both sites (Fig. 7a), with a higher daily flux value occurring during the cooling phase than during the warming phase of the year at the same temperature. The cooling phase occurred roughly between peak daily sediment temperature (roughly August 10th) and December 31st and warming phase between the January 1st to August 9th. The hysteresis was most evident when the temperature was between 15 and 25 °C (Table S4). The Q_{10} during the warming phase was 3.00 and 8.17 for the pond and the lake, respectively. The cooling phase exhibited lower Q_{10} values, specifically 1.95 for the pond and 3.25 for the lake. Similar trends were also captured at the monthly scale (Fig. 7b).

At our sites, the correlations between the seasonal mean CH_4 flux and NH-N, TP, DOC and DO concentrations were not significant, in part due to large scatter among a small sample size. In Fig. 8, we combine our seasonal data with data found in the published literature (Table S5) to explored the correlation between CH_4 flux and these water quality factors. A significant and positive relationship between CH_4 flux and $NH^{+}{}_{4}$-N and TN was found across the aquaculture systems (Fig. 8a–b). The correlation coefficient was 0.41 and 0.52 for $NH^{+}{}_{4}$-N and TN ($p < 0.05$), respectively. Although there was a trend of increasing CH_4 flux with higher DOC content, the correlation was not significant ($r = 0.25$, $p = 0.20$, Fig. 8c). Chl-a showed a robust positive correlation with CH_4 flux ($r = 0.61$, $p < 0.05$, Fig. 8d).

4. Discussion

4.1. *Importance of high-resolution CH_4 measurements*

Understanding the temporal variability in CH_4 flux is crucial for developing effective sampling strategies and for gaining mechanistic understanding of CH_4 emission processes. This study covered a wide range of timescale, from the 10 Hz eddy timescale to diurnal and seasonal timescales. At the eddy timescale, the data carried the imprints of ebullition flux, allowing the total flux to be partitioned into ebullition and non-ebullition contributions.

At the diurnal scale, previous studies have reported large diurnal variations in CH_4 flux in unmanaged natural water bodies, but they disagree with regard to timing of the peak flux occurrence (Podgrajsek et al., 2014; Jammet et al., 2017; Zhang et al., 2019; Sieczko et al., 2020; Waldo et al., 2021; Hounshell et al., 2023). Using an automated chamber system, Sieczko et al. (2020) found that CH_4 flux at four dimictic lakes in the boreal and north temperate regions, with maximum water depths ranging from 4.5 m to 11 m, was, on average, 2.4 times higher during the day than at night. Other studies showed that the nighttime CH_4 flux exceeded the daytime flux by a factor of 1 to 3 in shallow ponds and shallow lakes (Podgrajsek et al., 2014; Jammet et al., 2017; Zhang et al.,

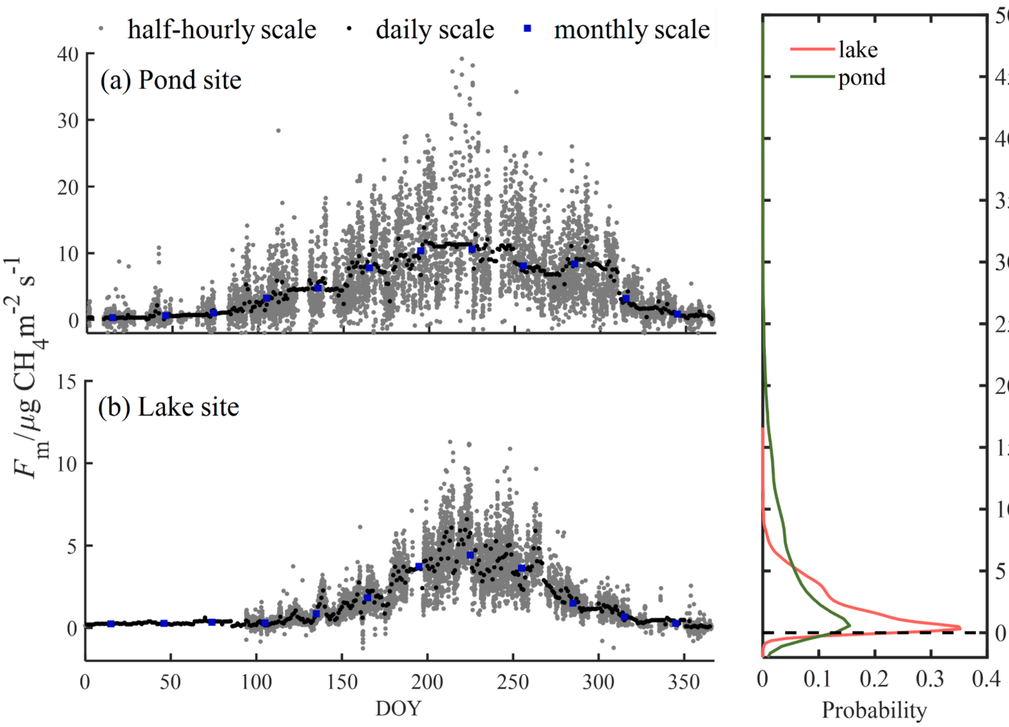

Fig. 5. (a-b) Temporal variations of CH_4 flux at three timescales: gray dots: half-hourly; black dots: daily; blue lines: monthly. (c) Probability density distribution of half-hourly CH_4 flux. (For interpretation of the references to colour in this figure legend, the reader is referred to the web version of this article.)

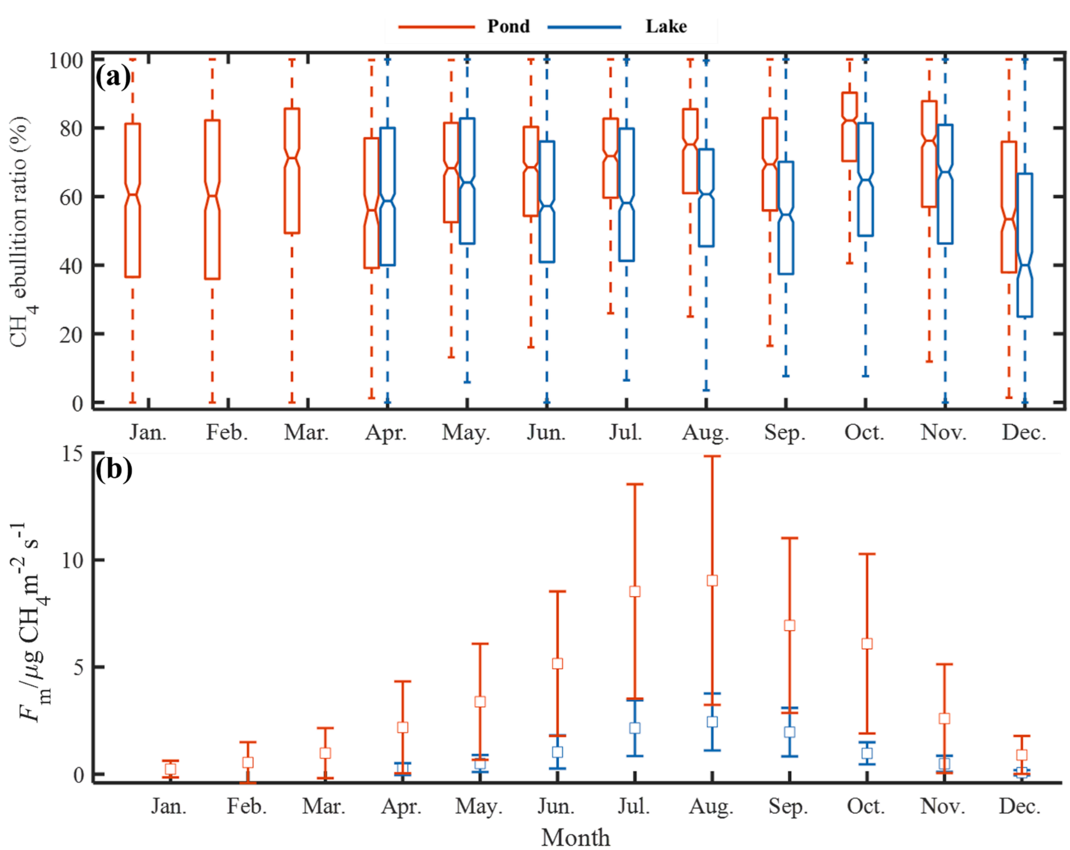

Fig. 6. (a) Boxplot of half-hourly CH_4 ebullition ratio. The notch, the lower boundary, and the upper boundary correspond to the median, the first quartile (25th percentile), and the third quartile (75th percentile), respectively, and the whiskers extend to ± 1.5 times the interquartile range. (b) Monthly mean CH_4 ebullitive rate, with error bars representing ± one standard deviation.

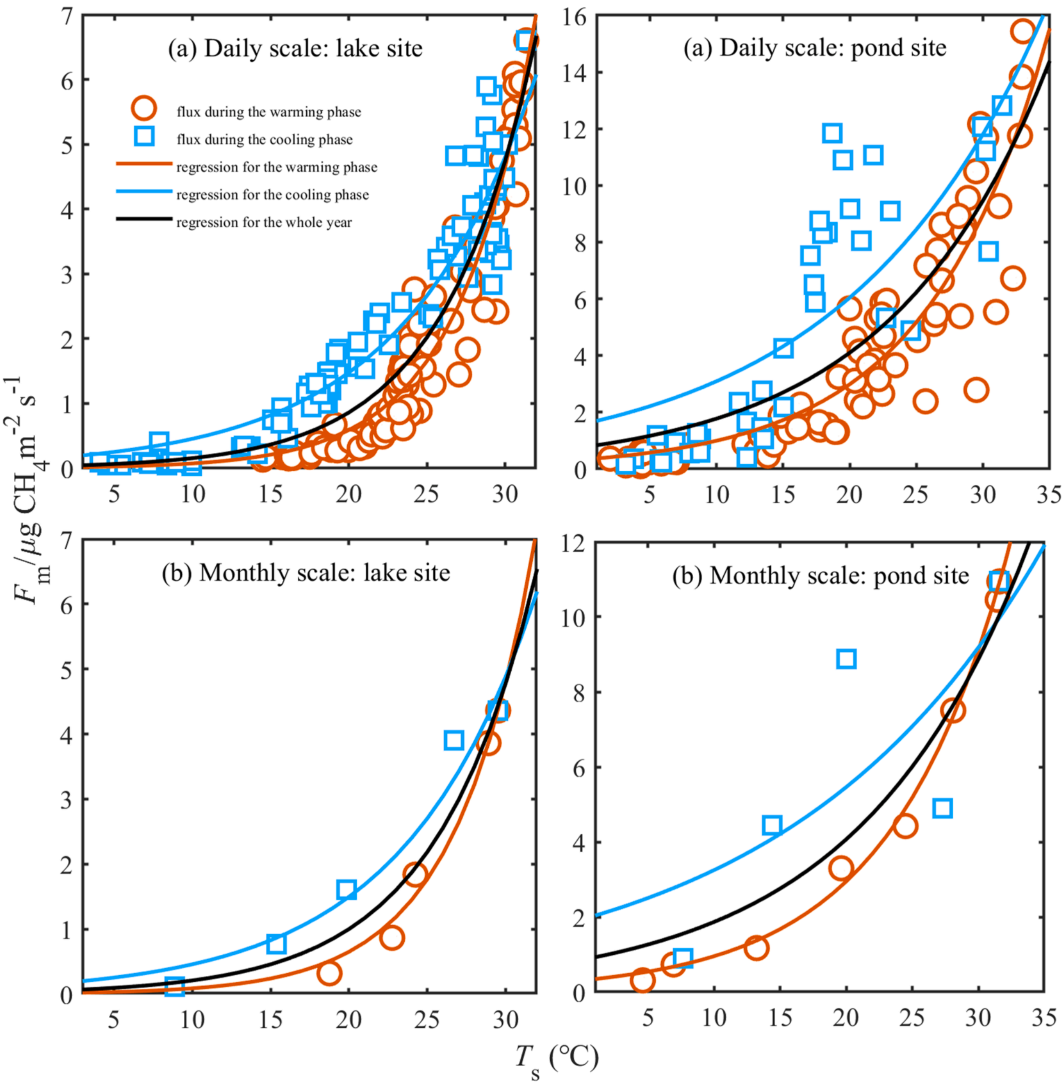

Fig. 7. (a) Relationship between CH_4 flux (F_m) and sediment temperature (T_s) at the daily and (b) monthly scale. Lines represent regression equations given in Table S4.

2019). These variations underscore the risk of over- or underestimating CH_4 flux when relying solely on daytime measurements to temporal extrapolation. In comparison to these unmanaged systems, our continuous, high-resolution observations showed less pronounced diurnal patterns at the two aquaculture systems. Averaged over the year, the difference between the daytime flux and the nighttime flux was 4 % for the pond and − 9 % for the lake. Given that most studies in aquaculture systems have predominantly concentrated their sampling between 09:00 to 12:00 (Kosten et al., 2020; Yang et al., 2024), our findings imply a potential 6 % to 8 % bias in the annual CH_4 emission estimate if only daytime data are used.

At multi-day to seasonal timescales, the total CH_4 flux and the ebullitive flux were characterized by peaks in the warm season and low values in the cold season at both sites. The seasonal pattern was consistent with those observed in other aquaculture systems (Tong et al., 2021; Yang et al., 2020; Yang et al., 2023; Yuan et al., 2021; Fang et al., 2022; Zhang et al., 2022a). In line with Wik et al. (2016), the diurnal variability in CH_4 flux at our sites was weaker than the day-to-day variability, with the daily flux varying by over 10 times in the same season. This significant day-to-day fluctuation, rather than diurnal changes, is likely the main source of large uncertainty in past CH_4 flux estimates, which often relied on sparse observations spread out over the year or short-term (a few weeks) campaigns. Our results show a notable reduction in the standard deviation of the annual flux as sampling duration increases (Fig. S1). Here we conducted a bootstrap analysis to evaluate the effect of various sampling scenarios on the annual CH_4 emission estimates (Fig. 9). In our analysis, we define the "chance of high-accuracy flux estimates" as the fraction of estimates that fall within ± 20 % of the observed annual mean. For example, for the annual mean value is 1.52 μg CH_4 m^{-2} s^{-1}, a high-accuracy flux estimate would be any value between 1.22 μg CH_4 m^{-2} s^{-1} and 1.82 μg CH_4 m^{-2} s^{-1}. A 100 % probability indicates that all estimates based on a certain sampling scenarios fall within this range. Conversely, a 0 % probability would indicate that none of the estimates fall within this range. Drawing upon the insights from Wik et al. (2016), we propose a minimum sampling duration of 80 days for pond aquaculture and 120 days for lake aquaculture, evenly distributed throughout the year, to ensure accurate CH_4 emission estimates (Fig. 9).

4.2. Annual CH_4 emission

We show that the pond and the lake were large sources of atmospheric CH_4, with the annual flux of 120 g CH_4-C m^{-2} yr^{-1} and 36 g CH_4-C m^{-2} yr^{-1}, respectively. These flux levels are three to eight times greater than the median annual fluxes from inland (unmanaged) waterbodies reported in a recent synthesis study utilizing EC

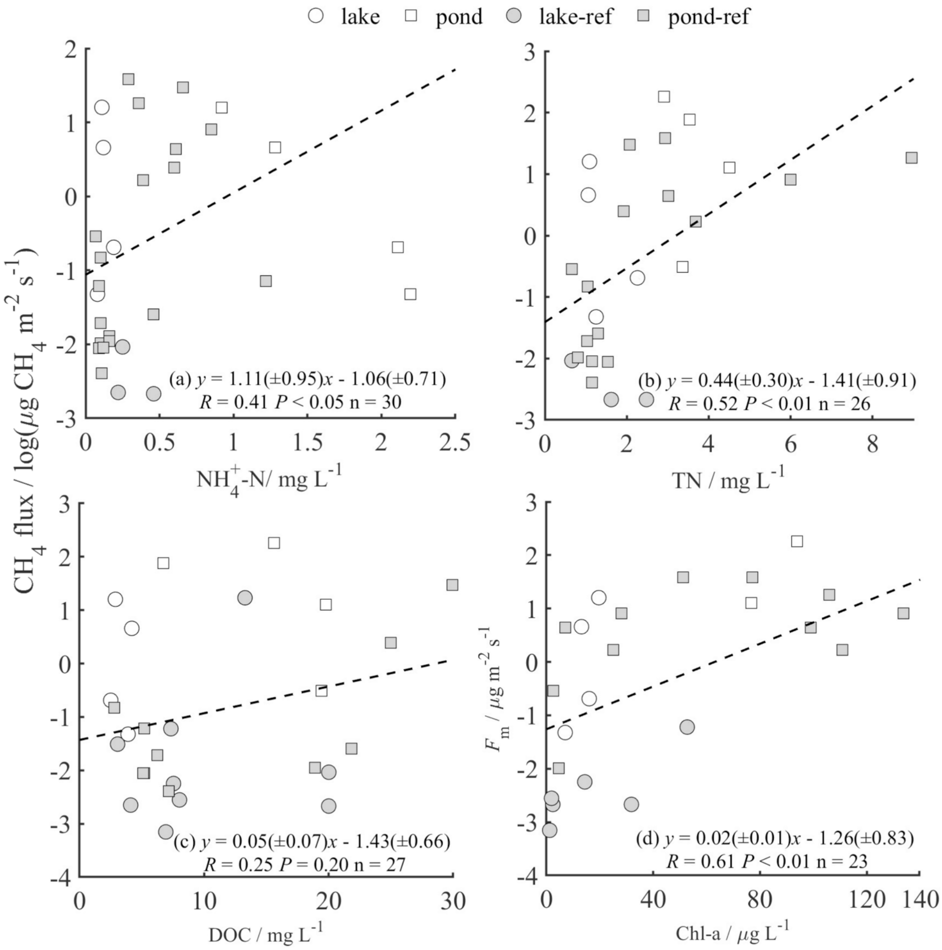

Fig. 8. Relationships between CH_4 flux and (a) $NH^{+}{}_{4}$.N concentration, (b) TN concentration, (c) DOC concentration, and (d) Chl-a concentration. Open symbols denote seasonal observed data at our sites, while closed symbols denote data in other published studies on aquacultural systems, representing the annual mean values for each system (Supplementary Table S5 and S6).

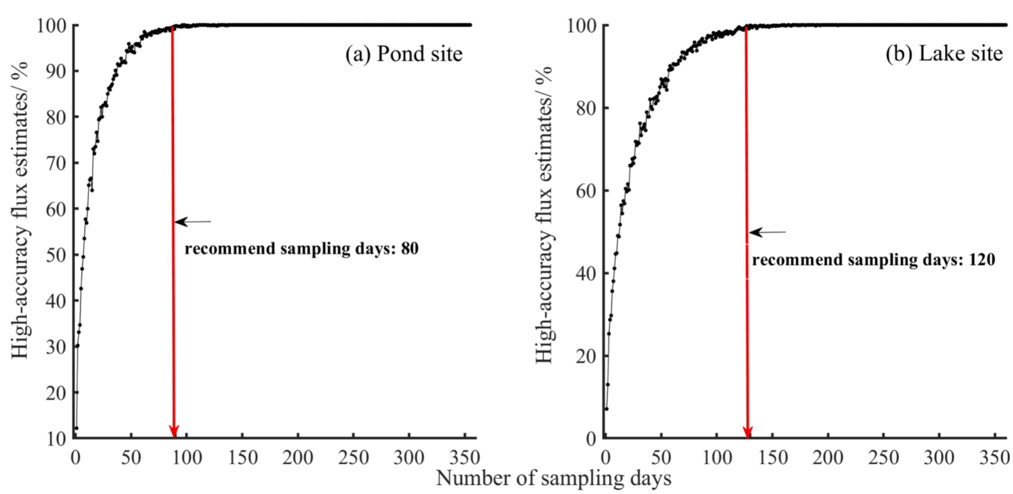

Fig. 9. Probability of achieving high-accuracy CH_4 flux estimates as a function of the number of sampling days for pond (a) and lake (b) site. Arrows indicate the sampling days required for a 95 % confidence level in estimating fluxes within ± 20 % of the observed annual mean.

measurements (Knox et al., 2019). They exceed the annual emissions in other ecological zones of Lake Taihu (eutrophic zone: 1.35 g CH_4-C m^{-2} yr^{-1}; submerged vegetation zone: 6.12 g CH_4-C m^{-2} yr^{-1}; Xiao et al., 2014b; Zhang et al., 2019) by one to two orders of magnitude. According to the *meta*-analysis provided by Zhang et al. (2022d), Zhang et al. (2024), the annual CH_4 flux from aquaculture pond is also substantially higher than those of other aquaculture systems regardless of size or waterbody/wetland types. Specifically, the CH_4 emissions from other aquaculture systems are 88 g CH_4-C m^{-2} yr^{-1} with size smaller than 1 ha and 27 g CH_4-C m^{-2} yr^{-1} with size larger than 1 ha; For waterbody/

wetland types used for aquaculture, the CH_4 emissions reported by these authors are 80 g CH_4-C m^{-2} yr^{-1} (ditches), 60 g CH_4-C m^{-2} yr^{-1} (paddy fields), 5 g CH_4-C m^{-2} yr^{-1} (reservoirs), and 3 g CH_4-C m^{-2} yr^{-1} (lakes). We also note that our pond and the lake values bracket those reported for ecosystems heavily impacted by human activities and using multi-years EC observation, such as small eutrophic reservoirs (42 g CH_4-C m^{-2} yr^{-1}; Waldo et al., 2021) and rice paddies (42 g CH_4-C m^{-2} yr^{-1}, Liu et al., 2023; 60 g CH_4-C m^{-2} yr^{-1}, Zhang et al., 2024).

The IPCC emission factor for fish aquaculture is 183 kg CH_4 ha^{-1} yr^{-1} or 13.7 g CH_4-C m^{-2} yr^{-1}. However, our study revealed the CH_4 EF was not uniform across different aquaculture types within the same climate zone. Specifically, both sites showed EFs significantly higher than the IPCC default value, with the pond being 8.8 times higher and the lake site 2.6 times higher. This finding is consistent with the *meta*-analysis results, which show that different aquaculture types produce varying amounts of CH_4 (Yuan et al., 2019; Dong et al., 2022; Zhang et al., 2022d; Zhang et al., 2024). Additionally, we also observed large temporal variations in EF values at both sites, with differences ranging from 4.5 to 7 times between the aquaculture period (April to November) and non-aquaculture period (January to March and December). These results suggest that using a single EF for all aquaculture types and period in CH_4 budget accounting may be inappropriate.

4.3. Role of ebullition

The high CH_4 emissions in our aquaculture systems were largely linked to the high ebullition ratio. Previous studies have established the dominant role of CH_4 ebullition in the total CH_4 emission from inland aquatic ecosystems. Generally, the ebullitive flux accounts for over 50 % of the total emission (e.g., Bastviken et al., 2008; Sawakuchi et al., 2014; Wu et al., 2019). In organic-rich shallow zones, the ebullition ratio can be as high as 98 % (DelSontro et al., 2016; Yang et al., 2020). Our results, from the EC partitioning method, corroborates this, revealing that ebullition contributes 60 % and 70 % of the total CH_4 flux at the lake and the pond, respectively. These high ebullition ratios can be attributed to factors that favor bubble formation and the subsequent CH_4 emission, such as low hydrostatic pressure, shallow water depths, and abundant organic inputs (Zhu et al., 2016; Fang et al., 2022).

In natural ecosystems, the ebullition ratio is size-dependent, typically with smaller water bodies showing higher ratios than larger ones (Bastviken et al., 2004; DelSontro et al., 2016). This size-dependence behavior was absent in this study. The two systems differ in size by several order of magnitudes (pond area 0.6 ha versus lake area 10600 ha), but their ebullition ratios were comparable. The size independence is also suggested by previous studies of aquaculture systems, where aquaculture sizes varied widely, from 0.09 ha to 2.7 ha, and ebullition ratios were consistently high, ranging between 80 % and 98 % (Yang et al., 2020; Yuan et al., 2021; Tong et al., 2021; Fang et al., 2022). In addition to size-dependence, water depth is a key factor influencing ebullition, with shallower waters showing higher flux rates than deeper ones (Bastviken et al., 2004; DelSontro et al., 2016). The two systems had similar water depth (lake: 1.3 m; pond: 1.8 m), which may be an explanation for this comparable ebullition ratio between the two systems.

4.4. Potential causes of high pond CH_4 emission

Significant differences in CH_4 emissions were observed between the pond and the lake aquaculture systems, with the pond system showing a threefold higher annual flux rate than the lake system. This disparity is consistent with findings from a *meta*-analysis by Zhang et al. (2022d), which reported substantial higher CH_4 emissions from pond aquaculture compared to lake and reservoir aquaculture. One key factor contributing to these higher CH_4 emissions is elevated nutrient loading in ponds (Dong et al., 2022; Yang et al., 2019, 2022, 2024b; Zhang et al., 2022d). Previous studies have highlighted the roles of allochthonous nutrient inputs and in-situ high productivity in enhancing CH_4 emissions in aquatic ecosystems (Rasilo et al., 2015; Sepulveda et al., 2018; Beaulieu et al., 2019; Wang et al., 2021; Zhang et al., 2023a) and some pristine lakes (Borges et al., 2022). In our study, the primary difference between the lake and the pond systems was the severity of human activities, given their similar climatic conditions. We hypothesize that the greater feed supply to the pond system (annual input: 8570 kg C/ha) compared to the lake system (annual input: 6400 kg C/ha) provided more substrates for methanogenesis, therefore driving higher CH_4 emissions.

Additionally, concentrations of TN and TP, which are indicators of anthropogenic nutrient input, are known to correlate with increased CH_4 emission by accelerating in-situ CH_4 production (Tang et al., 2021; Wu et al., 2023). Our findings support this relationship, with the pond system showing a threefold increase in TN and TP concentrations across all seasons compared to the lake system. Moreover, the concentration of $NH^+{}_4$.N, another marker of nutrient enrichment, likely contributed to CH_4 production and slowed CH_4 oxidation due to preferential oxidation by methane monooxygenase (Holmes et al., 1995; Xiao et al., 2020; Zhou et al., 2020). The 13-fold higher $NH^+{}_4$.N concentration in the pond system compared to the lake system further supports the assertion that nutrient enrichment, primarily from feed and animal waste application, substantially enhanced CH_4 emission in the pond system. This is further corroborated by the significant and positive relationships between CH_4 flux and TN as well as $NH^+{}_4$.N concentrations revealed by a *meta*-analysis (Fig. 8).

High phytoplankton biomass and high primary productivity are additional factors likely driving the high emission from the pond system. Previous research has identified Chl-a, an indicator of phytoplankton biomass and productivity, as a strong predictor of CH_4 emissions (Bastviken et al., 2004; Rasilo et al., 2015; Beaulieu et al., 2019). Elevated Chl-a concentrations can supply newly produced organic matter, providing the essential precursors for CH_4 production (Huttunen et al., 2003; Schroll et al., 2023). In this study, the Chl-a concentration was much higher in the pond system (85.0 μg L^{-1}) than in the lake system (17.8 μg L^{-1}), and we observed a strong positive correlation between CH_4 flux and the Chl-a concentration in both systems ($r = 0.61$, $p < 0.05$), supporting the notion that high Chl-a conditions are conducive to increased CH_4 emissions.

Another potential explanation for the high CH_4 emission from the pond system was its small size. Our findings, in agreement with previous studies (Holgerson and Raymond, 2016; Grinham et al., 2018; Zhang et al., 2022d), demonstrate that the size of water bodies plays a critical role in determining CH_4 flux. Smaller bodies are typically associated with higher CH_4 emissions due to their higher perimeter-to-area ratios and shallower depths, which enhance the retention of allochthonous organic carbon and decrease the likelihood of methane oxidation (Holgerson and Raymond, 2016). While lake aquaculture is characterized by larger open waters and greater water circulation, the more enclosed and stagnant conditions of ponds foster the accumulation of DOC and nutrients, creating favorable environment for methanogenesis. Indeed, our measurements revealed much higher DOC concentrations in the pond system (15.46 mg/L) than in the lake system (3.37 mg/L; Fig. 2e). Although the relationship between the DOC concentration and CH_4 flux was not statistically significant, higher CH_4 fluxes were observed during periods of elevated DOC concentrations in both aquaculture systems, suggesting that the size of a waterbody may regulate CH_4 emissions. Additionally, the CH_4 emissions recorded in our study exceeded the predictions of the area-dependent scaling relationship proposed by Holgerson and Raymond (2016) by two to three orders of magnitude. This discrepancy may be attributed to the substantial organic inputs typical of aquaculture systems, which act as a potent stimulant for CH_4 production. These findings highlight the importance of considering not only the size of the water body but also the specific conditions of the system when estimating annual CH_4 emissions.

4.5. Sensitivity of CH_4 flux to temperature

The significant exponential relationships between CH_4 flux and temperature, observed across varying time scales at both the pond and the lake site, underscores the important role of temperature in regulating CH_4 emissions in these aquaculture systems. This pattern aligns with findings across a wide range of ecosystems (Yvon-Durocher et al., 2014; Aben et al., 2017; DelSontro et al., 2018; Jansen et al., 2020). However, unlike previous studies, our high-resolution in-situ measurements at both the pond and the lake aquaculture systems revealed the presence of a “hysteretic effect” – a phenomenon where the sensitivity of CH_4 flux to temperature varies throughout the year (Davidson et al., 2018; Kariyapperuma et al., 2018; Jansen et al., 2020; Bao et al., 2021; Chang et al., 2020; Chang et al., 2021). Specifically, CH_4 flux was higher during the cooling phase of the year compared to the warming phase at the same temperature. This was likely due to increased substrate availability from unused feed material and phytoplankton accumulation during the cooling phase, which simulates methanogenesis (Chang et al., 2020; Chang et al., 2021).

Considering the strong temperature dependence of CH_4 flux, temperature is commonly used as a predictor for estimating annual CH_4 emissions in various ecosystems (Aben et al., 2017; Jansen et al., 2020). However, assuming a static relationship between temperature and CH_4 flux could lead to large uncertainties. For instance, during the warming phase, CH_4 flux could be overestimated by 14 % at the lake site and 20 % at the pond site, while during the cooling phase, underestimations could range between 17 % and 30 %. Such large seasonal biases highlight the importance of incorporating the seasonal hysteretic dynamics into predictive models to improve the accuracy of CH_4 emission estimates in diverse aquaculture systems.

This study also identified a notable difference in the temperature sensitivity (Q_{10}) of CH_4 emissions between the lake and the pond aquaculture systems. The lake system exhibited a high Q_{10} of 5.75, which exceeds the global wetland average Q_{10} of 2.23 based on EC measurements in 47 wetlands (Delwiche et al., 2021). In contrast, the pond system’s Q_{10} of 2.29 closely aligned with the global average, indicating a more moderate response to temperature fluctuations. The difference in Q_{10} values between these two aquaculture systems is likely due to the more pronounced impact of nutrient enrichment on CH_4 emissions in lake systems. This nutrient enrichment can amplify the temperature’s role in CH_4 production, as suggested by long-term mesocosm studies (Davidson et al., 2015). High temperature sensitives have also been observed in other aquatic ecosystems, including boreal lakes, northern ponds, urban ponds, rivers, and streams (Rasilo et al., 2015; DelSontro et al., 2016; Rocher-Ros et al., 2023; Bauduin et al., 2024).

These findings underscore the need for a comprehensive approach that accounts both biotic factors (e.g., nutrient loading) and abiotic factors (e.g, temperature) to accurately predict CH_4 emission in aquaculture systems. Future research should focus on the complex interactions between temperature, nutrient loading, and eutrophication, and how they collectively regulate CH_4 emissions across various aquaculture settings.

4.6. Implications of the present study

Several studies have explored variations in CH_4 emissions across different fish species, management practices, and measurement locations (Ma et al., 2018; Yang et al., 2019; Fang et al., 2022; Nijman et al., 2022; Zhang et al., 2022d; Znachor et al., 2023). However, less attention has been given to comparing different types of aquaculture system. Our study addresses this gap by comparing CH_4 flux between two major systems – lake-based and pond-based – in the YRD, China.

The substantial differences in CH_4 flux between the two systems underscore the need for type-specific investigations. Currently, a major transition from lake to pond aquaculture is under way, driven by local policy initiatives. Using the total lake aquaculture area (688,500 ha) in China in 2020 and the difference in the annual flux rate of 840 kg CH_4-C/ha between the pond and the lake, our findings suggest that replacing all lake aquaculture systems with pond-based ones would increase CH_4 emission by 0.6 Tg CH_4-C per year. This represents a 30 % rise from the current national freshwater aquaculture systems total of 1.9 Tg CH_4-C per year (Zhang et al., 2024). Although this transition accounts for a relatively small percentage (1 %) of the country’s total CH_4 emissions (49 Tg CH_4-C yr^{-1}, Chen et al., 2022), it underscores the environmental trade-offs involved in different aquaculture system types and stresses the need for a balanced approach that integrates economic, ecological, and climate considerations.

As with many other studies, this work has some limitations. First, while our results corroborate previous research showing that aquaculture systems are large sources of atmospheric CH_4 (Yuan et al., 2019; Tong et al., 2021; Zhao et al., 2021; Yang et al., 2024), we also found that the transition from lake aquaculture to pond aquaculture could result in a threefold increase in CH_4 emission. This finding bridges a knowledge gap and provides empirical data that can help refine emission inventories. However, the influence of management practices (aeration, drainage, and dredging) requires further exploration.

Second, our study focused a one-year observation period. Previous studies have demonstrated considerable inter-annual variability in CH_4 emissions (Fang et al., 2022; Yang et al., 2024). Longer-term, multi-year observations are necessary for a more accurate comparison between the lake and the pond aquaculture systems.

Last, the field measurements in this study were limited to a specific region and climate, and specific fish species. Despite the high-frequency observations with identical instrumentation, the conclusions drawn from the comparison of one lake and one pond may lack sufficient generalizability to represent broader aquaculture systems. To improve the accuracy of CH_4 estimation at these larger scales, further comparative pond-lake studies should focus on diverse locations, climate, and aquaculture practices.

5. Conclusions

This study presents the first comparative analysis of CH_4 flux from lake and pond aquaculture systems, based on simultaneous one-year eddy covariance measurements. Results show minimal diurnal variability in CH_4 flux at both sites, but large day-to-day variability, underscoring the need for high-frequency observations to capture these fluctuations. Both pond and lake aquaculture farms were large CH_4 sources, with annual rates of 120 g CH_4-C m^{-2} yr^{-1} for the pond system and 36 g CH_4-C m^{-2} yr^{-1} for the lake system. The three-fold increase in CH_4 emission from the lake to the pond aquaculture highlights the importance of considering type-specific differences when assessing aquaculture-related CH_4 emissions. The higher CH_4 flux in the pond system was likely driven by a combination of biotic factors, such as high nutrient and carbon loadings and Chl-a concentration, and abiotic factors like the smaller surface area and stagnant conditions compared to the lake.

Our findings showed that sediment temperature was a key driver of CH_4 flux variability across multiple time scales (half-hourly, daily, and monthly) in both systems. Intriguingly, we observed an asymmetric response of CH_4 flux to sediment temperature at both sites: the flux was higher during the cooling phase compared to the warming phase at the same temperature. Additionally, the pond site exhibited a lower Q_{10} value than the lake site, possibly due to the dampening effect of high nutrient loading on temperature sensitivity.

CRediT authorship contribution statement

Jiayu Zhao: Writing – original draft, Funding acquisition, Formal analysis, Data curation, Conceptualization. **Mi Zhang:** Data curation. **Yini Pu:** Methodology, Data curation. **Lei Jia:** Data curation. **Wei Xiao:** Funding acquisition, Data curation. **Zhen Zhang:** Data curation. **Pei Ge:**

Data curation. **Jie Shi:** Data curation. **Qitao Xiao:** Writing – review & editing, Funding acquisition, Data curation. **Xuhui Lee:** Writing – review & editing, Data curation, Conceptualization.

Declaration of competing interest

The authors declare that they have no known competing financial interests or personal relationships that could have appeared to influence the work reported in this paper.

Acknowledgements

This research was supported jointly by the Natural Science Foundation of Jiangsu Province for Distinguished Young Scholars (BK20220055), the National Natural Science Foundation of China (no. 42401111, 42271114, 42021004), the Provincial Science and Technology Innovative Program for Carbon Peak and Carbon Neutrality of Jiangsu of China (BE2022422), the R&D Foundation of Jiangsu Province, China (BK20220020), the National Key R&D Program of China (2020YFA0607501), the "333 Project" of Jiangsu Province (BRA20222023), the Youth Innovation Promotion Association of CAS (2023329) and the Program for scientific research startup funds of Guangdong Ocean University (060302032302).

Appendix A. Supplementary data

Supplementary data to this article can be found online at https://doi.org/10.1016/j.jhydrol.2025.132765.

Data availability

Data will be made available on request.

References

Aben, R.C., Barros, N., Van Donk, E., Frenken, T., Hilt, S., Kazanjian, G., Lamers, L.P., Peeters, E.T., Roelofs, J.G., Domis, L.N., Stephan, S., Velthuis, M., Wall, D.B., Wik, M., Thornton, B.F., Wilkinson, J., DelSontro, T., Kosten, S., 2017. Cross continental increase in methane ebullition under climate change. Nat. Commun. 8 (1), 1682. https://doi.org/10.1038/s41467-017-01535-y.

Bao, T., Xu, X.Y., Jia, G.S., Billesbach, D.P., Sullivan, R.C., 2021. Much stronger tundra methane emissions during autumn freeze than spring thaw. Global Change Biol. 27 (2), 376–387.

Bastviken, D., Cole, J., Pace, M., Tranvik, L., 2004. Methane emissions from lakes: dependence of lake characteristics, two regional assessments, and a global estimate. Global Biogeochem. Cy. 18, GB4009. https://doi.org/10.1029/2004GB002238.

Bastviken, D., Cole, J.J., Pace, M.L., Van de Bogert, M.C., 2008. Fates of methane from different lake habitats: connecting whole-lake budgets and CH_4 emissions. J. Geophys. Res. 113, G02024. https://doi.org/10.1029/2007JG000608.

Bauduin, T., Gypens, N., Bores, A.V., 2024. Methane, carbon dioxide and nitrous oxide emissions from two clear-water and two turbid-water urban ponds in Brussels (Belgium). Biogeosciences Discussion. https://doi.org/10.5194/egusphere-2024-1315.

Beaulieu, J.J., DelSontro, T., Downing, J.A., 2019. Eutrophication will increase methane emissions from lakes and impoundments during the 21st century. Nat. Commun. 10 (1), 1375. https://doi.org/10.1038/s41467-019-09100-5.

Borges, A.V., Abril, G., Darchambeau, F., Teodoru, R.C., Deborde, J., Vidal, O.L., Lambert, T., Bouillon, S., 2015. Divergent biophysical controls of aqutic CO_2 and CH_4 in the World's two largest rivers. Sci Rep 5, 15614. https://doi.org/10.1038/srep15614.

Borges, A.V., Deirmendjian, L., Bouillon, S., Okello, W., Lambert, T., Roland, F.A.E., Razanamahandry, V.F., Voarintsoa, N.R.G., Darchambeau, F., Kimirei, I.A., Descy, J.-P., Allen, G.H., Morana, C., 2022. Greenhouse gas emissions from African lakes are no longer a blind spot. eabi8716 Sci. Adv. 8, 1–17. https://doi.org/10.1126/sciadv.abi8716.

Cao, L., Naylor, R., Henriksson, P., Leadbitter, D., Metian, M., Troell, M., Zhang, W.B., 2015. China's aquaculture and the world's wild fisheries. Science 347, 133–135. https://doi.org/10.1126/science.126014.

Chang, K.Y., Riley, W.J., Crill, P.M., Grant, R.F., Saleska, S.R., 2020. Hysteretic temperature sensitivity of wetland CH_4 fluxes explained by substrate availability and microbial activity. Biogeosciences 17 (22), 5849–5860. https://doi.org/10.5194/bg-17-5849-2020.

Chang, K.Y., Riley, W.J., Knox, S.H., Jackson, R.B., McNicol, G., Poulter, B., Zona, D., 2021. Substantial hysteresis in emergent temperature sensitivity of global wetland CH_4 emissions. Nat. Commun. 12 (1), 2266. https://doi.org/10.1038/s41467-021-22452-1.

Chen, Z.C., Jacob, D.J., Nesser, H., Sulprizio, P.M., Lorente, A., Varon, J.D., Lu, X., Shen, L., Qu, Z., Penn, E., Yu, X.Y., 2022. Methane emissions from China: a high-resolution inversion of TROPOMI satellite observations. Atmos. Chem. Phys. 22, 10809–10826. https://doi.org/10.5194/acp-22-10809-2022.

Chen, G.Z., Bai, J.H., Bi, C., Wang, Y.Q., Cui, B.S., 2023. Global greenhouse gas emissions from aquaculture: a bibliometric analysis. Agr. Ecosyst. Environ. 348, 108405. https://doi.org/10.1016/j.agee.2023.108405.

China Fishery Statistical Yearbook, 2023. China Agriculture Press, Beijing.

Davidson, T.A., Audet, J., Svenning, J.C., Lauridsen, T.L., Søndergaard, M., Landkildehus, F., Larsen, S.E., Jeppesen, E., 2015. Eutrophication effects on greenhouse gas fluxes from shallow-lake mesocosms override those of climate warming. Global Change Biol. 21 (12), 4449–4463. https://doi.org/10.1111/gcb.13062.

Davidson, T.A., Audet, J., Jeppesen, E., Landkildehus, F., Lauridsen, T.L., Søndergaard, M., Syväranta, J., 2018. Synergy between nutrients and warming enhances methane ebullition from experimental lakes. Nat. Clim. Change. 8 (2), 156–160. https://doi.org/10.1038/s41558-017-0063-z.

DelSontro, T., Beaulieu, J.J., Downing, J.A., 2018. Greenhouse gas emissions from lakes and impoundments: Upscaling in the face of global change. Limnology and Oceanography Letters 3 (3), 64–75.

DelSontro, T., Boutet, L., St-Pierre, A., del Giorgio, P.A., Prairie, Y.T., 2016. Methane ebullition and diffusion from northern ponds and lakes regulated by the interaction between temperature and system productivity. Limnol. Oceanogr. 61 (S1), S62–S77. https://doi.org/10.1002/lno.10335.

Delwiche, K.B., Knox, S.H., Malhotra, A., Fluet-Chouinard, E., McNicol, G., Feron, S., Jackson, R.B., 2021. FLUXNET-CH_4: A global, multi-ecosystem dataset and analysis of methane seasonality from freshwater wetlands. Earth System Science Data Discussions 1–111. https://doi.org/10.5194/essd-13-3607-2021.

Dong, B.G., Xi, Y., Cui, Y.X., Peng, S.S., 2022. Quantifying methane emissions from aquaculture ponds in China. Environ. Sci. Technol. 57 (4), 1576–1583. https://doi.org/10.1021/acs.est.2c05218.

Duan, H.T., Xiao, Q.T., Qi, T.C., Hu, C., Zhang, M., Shen, M., Hu, Z.H., Wang, W., Xiao, W., Qiu, Y.G., Luo, J.H., Lee, X.H., 2023. Quantification of Diffusive Methane Emissions from a Large Eutrophic Lake with Satellite Imagery. Environ. Sci. Technol. 57 (36), 13520–13529. https://doi.org/10.1021/acs.est.3c05631.

Eugster, W., DelSontro, T., Sobek, S., 2011. Eddy covariance flux measurements confirm extreme CH_4 emissions from a Swiss hydropower reservoir and resolve their short-term variability. Biogeosciences 8 (9), 2815–2831. https://doi.org/10.5194/bg-8-2815-2011.

Fang, X.T., Wang, C., Zhang, T.R., Zheng, F.W., Zhao, J.T., Wu, S., Barthel, M., Six, J., Zou, J.W., Liu, S.W., 2022. Ebullitive CH_4 flux and its mitigation potential by aeration in freshwater aquaculture: Measurements and global data synthesis. Agr. Ecosyst. Environ. 335, 108016. https://doi.org/10.1016/j.agee.2022.108016.

Food and Agriculture Organization of the United Nations (FAO), 2022. The state of world fisheries and aquaculture 2022: Towards blue transformation. Rome, Italy. https://doi.org/10.4060/cc0461en.

Gephart, J.A., Henriksson, P.J., Parker, R.W., Shepon, A., Gorospe, K.D., Bergman, K., Eshel, G., Gloden, C.D., Halpern, B.S., Hornborg, S., Jonell, M., Metian, M., Mifflin, K., Newton, R., Tyedmers, P., Zhang, W.B., Ziegler, F., Troell, M., 2021. Environmental performance of blue foods. Nature 597 (7876), 360–365. https://doi.org/10.1038/s41586-021-03889-2.

Grinham, A., Albert, S., Deering, N., Dunbabin, M., Bastviken, D., Sherman, B., Lovelock, C.E., Evans, C.D., 2018. The importance of small artificial water bodies as sources of methane emissions in Queensland, Australia. Hydrol. Earth Syst. Sci. 22 (10), 5281–5298. https://doi.org/10.5194/hess-22-5281-2018.

Holmes, A.J., Costello, A., Lidstrom, M.E., Murrell, J.C., 1995. Evidence that participate methane monooxygenase and ammonia monooxygenase may be evolutionarily related. FEMS Microbiol. Lett 132 (3), 203–208. https://doi.org/10.1111/j.1574-6968.1995.tb07834.x.

Horst, T.W., Lenschow, D.H., 2009. Attenuation of scalar fluxes measured with spatially-displaced sensors. Boundary-Layer Meteorol 130, 275–300. https://doi.org/10.1007/s10546-008-9348-0.

Hounshell, A.G., D'Acunha, B.M., Breef-Pilz, A., Johnson, M.S., Thomas, R.Q., Carey, C. C., 2023. Eddy covariance data reveal that a small freshwater reservoir emits a substantial amount of carbon dioxide and methane. J Geophys Res-Biogeo 128 (3), e2022JG007091. https://doi.org/10.1029/2022JG007091.

Holgerson, M.A., Raymond, P.A., 2016. Large contribution to inland water CO_2 and CH_4 emissions from very small ponds. Nat. Geosci 9 (3), 222–226. https://doi.org/10.1038/ngeo2654.

Hu, B.B., Xu, X.F., Zhang, J.J., Wang, T.L., Meng, W.Q., Wang, D.Q., 2020. Diurnal variations of greenhouse gases emissions from reclamation mariculture ponds. Estuar Coast Shelf S 237, 106677. https://doi.org/10.1016/j.ecss.2020.106677.

Hwang, Y., Ryu, Y., Huang, Y., Kim, J., Iwata, H., Kang, M., 2020. Comprehensive assessments of carbon dynamics in an intermittently-irrigated rice paddy. Agri Forest Meteorol 285, 107933. https://doi.org/10.1016/j.agrformet.2020.107933.

Huttunen, J.T., Alm, J., Liikanen, A., Juutinen, S., Larmola, T., Hammar, T., Silvola, J., Martikainen, P.J., 2003. Fluxes of methane, carbon dioxide and nitrous oxide in boreal lakes and potential anthropogenic effects on the aquatic greenhouse gas emissions. Chemosphere 52 (3), 609–621. https://doi.org/10.1016/S0045-6535(03)00243-1.

IPCC, 2021. Summary for Policymakers. In: Masson-Delmotte, V., Zhai, P., Pirani, A., Connors, S.L., Péan, C., Berger, S., Caud, N., Chen, Y., Goldfarb, L., Gomis, M.I., Huang, M., Leitzell, K., Lonnoy, E., Matthews, J.B.R., Maycock, T.K., Waterfield, T., Yelekçi, O., Yu, R., Zhou, B. (Eds.), Climate Change 2021: the Physical Science Basis.

Contribution of Working Group I to the Sixth Assessment Report of the Intergovernmental Panel On Climate Change. Cambridge University Press, In Press.

Iwata, H., Hirata, R., Takahashi, Y., Miyabara, Y., Itoh, M., Iizuka, K., 2018. Partitioning eddy-covariance methane fluxes from a shallow lake into diffusive and ebullitive fluxes. Boundary-Layer Meteorol 169 (3), 413–428. https://doi.org/10.1007/s10546-018-0383-1.

Jammet, M., Dengel, S., Kettner, E., Parmentier, F.J.W., Wik, M., Crill, P., Friborg, T., 2017. Year-round CH_4 and CO_2 flux dynamics in two contrasting freshwater ecosystems of the subarctic. Biogeosciences 14 (22), 5189–5216. https://doi.org/10.5194/bg-14-5189-2017.

Jansen, J., Thornton, B.F., Wik, M., MacIntyre, S., Crill, P.M., 2020. Temperature proxies as a solution to biased sampling of lake methane emissions. Geohpys Res Lett 47 (14), e2020GL088647. https://doi.org/10.1029/2020GL088647.

Kariyapperuma, K.A., Johannesson, G., Maldaner, L., VanderZaag, A., Gordon, R., Wagner-Riddle, C., 2018. Year-round methane emissions from liquid dairy manure in a cold climate reveal hysteretic pattern. Agr Forest Meteorol 258, 56–65. https://doi.org/10.1016/j.agrformet.2017.12.185.

Kim, Y., Johnson, M.S., Knox, S.H., Black, T.A., Dalmagro, H.J., Kang, M., Baldocchi, D., 2020. Gap-filling approaches for eddy covariance methane fluxes: A comparison of three machine learning algorithms and a traditional method with principal component analysis. Global Change Biol 26 (3), 1499–1518. https://doi.org/10.1111/gcb.14845.

Knox, S.H., Jackson, R.B., Poulter, B., McNicol, G., Fluet-Chouinard, E., Zhang, Z., Zona, D., 2019. FLUXNET-CH_4 synthesis activity: Objectives, observations, and future directions. Bull Amer Meteor Soc. 100 (12), 2607–2632. https://doi.org/10.1175/BAMS-D-18-0268.1.

Kosten, S., Almeida, R.M., Barbosa, I., Mendonça, R., Muzitano, I.S., Oliveira-Junior, E. S., Vroom, R.J., Wang, H.J., Barros, N., 2020. Better assessments of greenhouse gas emissions from global fish ponds needed to adequately evaluate aquaculture footprint. Sci. Total Environ. 748, 141247. https://doi.org/10.1016/j.scitotenv.2020.141247.

Lee, X.H., Massman, W., Law, B., 2004. Handbook of Micrometeorology: A Guide for Surface Flux Measurement and Analysis, Vol. 29. Springer Science & Business Media.

Liu, X., Dai, X., Yang, F., Meng, S., Wang, H., 2023. CH_4 emissions from a double-cropping rice field in subtropical China over seven years. Agr Forest Meteorol 339, 109578. https://doi.org/10.1016/j.agrformet.2023.109578.

Ma, Y.C., Sun, L.Y., Liu, C.Y., Yang, X.Y., Zhou, W., Yang, B., Schwenke, G., Li Liu, D., 2018. A comparison of methane and nitrous oxide emissions from inland mixed-fish and crab aquaculture ponds. Sci. Total Environ. 637, 517–523. https://doi.org/10.1016/j.scitotenv.2018.05.040.

Mahabbati, A., Beringer, J., Leopold, M., McHugh, I., Cleverly, J., Isaac, P., Izady, A., 2021. A comparison of gap-filling algorithms for eddy covariance fluxes and their drivers. Geoscientific Instrumentation, Methods and Data Systems 10 (1), 123–140. https://doi.org/10.5194/gi-10-123-2021.

Mauder, M., Foken, T., 2004. Documentation and Instruction Manual of the Eddy Covariance Software Package TK2. University of Bayreuth. Department of Micrometeorology. Arbeitsergebnisse Nr. 26, 42.

McDermitt, D., Burba, G., Xu, L., Anderson, T., Komissarov, A., Riensche, B., Schedlbauer, J., Starr, G., Zona, D., Oechel, W., Oberbauer, S., Hastings, S., 2011. A new low-power, open-path instrument for measuring methane flux by eddy covariance. Appl. Phys. B 102 (2), 391–405. https://doi.org/10.1007/s00340-010-4307-0.

Moncrieff, J.B., Massheder, J.M., De Bruin, H., Elbers, J., Friborg, T., Heusinkveld, B., Kabat, P., Scott, S., Søgaard, H., Verhoef, A., 1997. A system to measure surface fluxes of momentum, sensible heat, water vapour and carbon dioxide. J. Hydrol. 188, 589–611. https://doi.org/10.1016/S0022-1694(96)03194-0.

Natchimuthu, S., Sundgren, I., Gålfalk, M., Klemedtsson, L., Crill, P., Danielsson, Å., Bastviken, D., 2016. Spatio-temporal variability of lake CH_4 fluxes and its influence on annual whole lake emission estimates. Limnol Oceanogr 61 (S1), S13–S26. https://doi.org/10.1002/lno.10222.

Naylor, R.L., Hardy, R.W., Buschmann, A.H., Bush, S.R., Cao, L., Klinger, D.H., Klinger, D.H., Little, D.C., Lubchenco, J., Shumway, S.E., Troell, M., 2021. A 20-year retrospective review of global aquaculture. Nature 591 (7851), 551–563. https://doi.org/10.1038/s41586-021-03308-6.

Nijman, T.P., Lemmens, M., Lurling, M., Kosten, S., Welte, C., Veraart, A.J., 2022. Phosphorus control and dredging decrease methane emissions from shallow lakes. Sci. Total Environ. 847, 157584. https://doi.org/10.1016/j.scitotenv.2022.157584.

Podgrajsek, E., Sahlée, E., Rutgersson, A., 2014. Diurnal cycle of lake methane flux. J Geophys Res: Biogeo 119 (3), 236–248. https://doi.org/10.1002/2013JG002327.

Pu, Y.N., Zhang, M., Jia, L., Zhang, Z., Xiao, W., Liu, S.D., Zhao, J.Y., Xie, Y.H., Lee, X.H., 2022. Methane emission of a lake aquaculture farm and its response to ecological restoration. Agr Ecosyst Environ 330, 107883. https://doi.org/10.1016/j.agee.2022.107883.

Qin, B.Q., Xu, P.Z., Wu, Q.L., Luo, L.C., Zhang, Y.L., 2007. Environmental issues of Lake Taihu, China. Hydrobiologia 581, 3–14. https://doi.org/10.1007/s10750-006-0521-5.

Rasilo, T., Prairie, Y.T., del Giorgio, P.A., 2015. Large-scale patterns in summer diffusive CH_4 fluxes across boreal lakes, and contribution to diffusive C emissions. Global Change Biol. 21 (3), 1124–1139. https://doi.org/10.1111/gcb.12741.

Rosentreter, J.A., Borges, A.V., Deemer, B.R., Holgerson, M.A., Liu, S.D., Song, C.L., Melack, J., Raymond, P.A., Duarte, C.M., Allen, G.H., Olefeldt, D., Poulter, B., Battin, T.I., Eyre, B.D., 2021. Half of global methane emissions come from highly variable aquatic ecosystem sources. Nat. Geosci. 14, 225–230. https://doi.org/10.1038/s41561-021-00715-2.

Rocher-Ros, G., Stanley, E.H., Loken, L.C., Casson, N.J., Raymond, P.A., Liu, S.D., Amatulli, A., Sponseller, R.A., 2023. Global methane emissions from rivers and streams. Nature 621 (7979), 530–535. https://doi.org/10.1038/s41586-023-06344-6.

Sawakuchi, H.O., Bastviken, D., Sawakuchi, A.O., Krusche, A.V., Ballester, M.V.R., Richey, J.E., 2014. Methane emissions from amazonian rivers and their contribution to the global methane budget. Global Change Biol. 20 (9), 2829–2840. https://doi.org/10.1111/gcb.12646.

Saunois, M., Martinez, A., Poulter, B., Zhang, Z., Raymond, P., Regnier, P., Zhuang, Q., 2024. Global Methane Budget 2000–2020. Earth Syst. sci. data Discuss. 2024, 1–147. https://doi.org/10.5194/essd-2024-115.

Schroll, M., Liu, L., Einzmann, T., Keppler, F., Grossart, H.P., 2023. Methane accumulation and its potential precursor compounds in the oxic surface water layer of two contrasting stratified lakes. Sci. Total Environ. 903, 166205. https://doi.org/10.1016/j.scitotenv.2023.166205.

Sepulveda-Jauregui, A., Hoyos-Santillan, J., Martinez-Cruz, K., Anthony, K.M.W., Casper, P., Belmonte-Izquierdo, Y., Thalasso, F., 2018. Eutrophication exacerbates the impact of climate warming on lake methane emission. Sci. Total Environ. 636, 411–419. https://doi.org/10.1016/j.scitotenv.2018.04.283.

Sieczko, A.K., Duc, N.T., Schenk, J., Pajala, G., Rudberg, D., Sawakuchi, H.O., Bastviken, D., 2020. Diel variability of methane emissions from lakes. P Natl Acad Sci Usa 117 (35), 21488–21494. https://doi.org/10.1073/pnas.2006024117.

Tang, W., Xu, Y.J., Ma, Y., Maher, D.T., Li, S.Y., 2021. Hot spot of CH_4 production and diffusive flux in rivers with high urbanization. Water Research 204, 117624. https://doi.org/10.1016/j.watres.2021.117624.

Tan, D., Li, Q., Wang, S.L., Yeager, K.M., Guo, M.W., Liu, K., Wang, Y.C., 2021. Diel variation of CH_4 emission fluxes in a small artificial lake: Toward more accurate methods of observation. Sci. Total Environ. 784, 147146. https://doi.org/10.1016/j.scitotenv.2021.147146.

Taoka, T., Iwata, H., Hirata, R., Takahashi, Y., Miyabara, Y., Itoh, M., 2020. Environmental controls of diffusive and ebullitive methane emissions at a sub-daily time scale in the littoral zone of a midlatitude shallow lake. J Geophys Res: Biogeo 125 (9), e2020JG005753. https://doi.org/10.1029/2020JG005753.

Thanwerdas, J., Saunois, M., Berchet, A., Pison, I., Bousquet, P., 2024. Investigation of the renewed methane growth post-2007 with high-resolution 3-D variational inverse modeling and isotopic constraints. Atmos. Chem. Phys. 24 (4), 2129–2167. https://doi.org/10.5194/acp-24-2129-2024.

Tong, C., Bastviken, D., Tang, K.W., Yang, P., Yang, H., Zhang, Y.F., Guo, Q.Q., Lai, D.Y., 2021. Annual CO_2 and CH_4 fluxes in coastal earthen ponds with Litopenaeus vannamei in southeastern China. Aquaculture 545, 737229. https://doi.org/10.1016/j.aquaculture.2021.737229.

Ueyama, M., Yazaki, T., Hirano, T., Endo, R., 2022. Partitioning methane flux by the eddy covariance method in a cool temperate bog based on a Bayesian framework. AGR FOREST METEOROL 316, 108852. https://doi.org/10.1016/j.agrformet.2022.108852.

Vickers, D., Mahrt, L., 1997. Quality control and flux sampling problems for tower and aircraft data. J Atmos Ocean Technol 14 (3), 512–526. https://doi.org/10.1175/1520-0426(1997)014.

Wang, B.H., Stirling, E., He, Z.L., Ma, B., Zhang, H.J., Zheng, X.F., Xiao, S.B., Yan, Q.Y., 2021. Pollution alters methanogenic and methanotrophic communities and increases dissolved methane in small ponds. Sci. Total Environ. 801, 149723. https://doi.org/10.1016/j.scitotenv.2021.149723.

Waldo, S., Beaulieu, J.J., Barnett, W., Balz, D.A., Vanni, M.J., Williamson, T., Walker, J. T., 2021. Temporal patterns and biophysical controls on methane emissions from a small eutrophic reservoir: insights from two years of eddy covariance monitoring. Biogeosciences Discussions 2021, 1–40. https://doi.org/10.5194/bg-2021-36.

Webb, E.K., Pearman, G.I., Leuning, R., 1980. Correction of flux measurements for density effects due to heat and water vapour transfer. Q. J. r. Meteorolog. Soc. 106 (447), 85–100. https://doi.org/10.1002/qj.49710644707.

Wik, M., Thornton, B.F., Bastviken, D., Uhlbäck, J., Crill, P.M., 2016. Biased sampling of methane release from northern lakes: A problem for extrapolation. Geophy Res Lett 43 (3), 1256–1262. https://doi.org/10.1002/2015GL066501.

Wu, S., Li, S.Q., Zou, Z.H., Hu, T., Hu, Z.Q., Liu, S.W., Zou, J.W., 2019. High methane emissions largely attributed to ebullitive fluxes from a subtropical river draining a rice paddy watershed in China. Environ. Sci. Technol. 53 (7), 3499–3507. https://doi.org/10.1021/acs.est.8b05286.

Wu, J., Lu, Y., Wang, H., Li, G., 2023. Effects of nitrogen and phosphorus additions on CH_4 flux in wet meadow of Qinghai-Tibet Plateau. Sci. Total Environ. 887, 163448. https://doi.org/10.1016/j.scitotenv.2023.163448.

Xiao, S.B., Yang, H., Liu, D.F., Zhang, C., Lei, D., Wang, Y.C., Peng, F., Li, Y.C., Wang, C. H., Li, X.L., Wu, G.C., Liu, L., 2014a. Gas transfer velocities of methane and carbon dioxide in a subtropical shallow pond. Tellus B 66 (1), 23795. https://doi.org/10.3402/tellusb.v66.23795.

Xiao, W., Liu, S.D., Li, H.C., Xiao, Q.T., Wang, W., Hu, Z.H., Hu, C., Gao, Y.Q., Shen, J., Zhao, X.Y., Zhang, M., Lee, X.H., 2014b. A flux-gradient system for simultaneous measurement of the CH_4, CO_2, and H_2O fluxes at a lake–air interface. Environ. Sci. Technol. 48 (24), 14490–14498. https://doi.org/10.1021/es5033713.

Xiao, Q.T., Zhang, M., Hu, Z.H., Gao, Y.Q., Hu, C., Liu, C., Liu, S.D., Zhang, Z., Zhao, J.Y., Xiao, W., Lee, X.H., 2017. Spatial variations of methane emission in a large shallow eutrophic lake in subtropical climate. J Geophys Res - Biogeo 122 (7), 1597–1614. https://doi.org/10.1002/2017JG003805.

Xiao, Q.T., Duan, H.T., Qi, T.C., Hu, Z.H., Liu, S.D., Zhang, M., Lee, X.H., 2020. Environmental investments decreased partial pressure of CO_2 in a small eutrophic urban lake: Evidence from long-term measurements. Environ Pollut 263, 114433. https://doi.org/10.1016/j.envpol.2020.114433.

Xiao, Q.T., Zhou, Y., Luo, J.H., Hu, C., Duan, H.T., Qiu, Y.G., Zhang, M., Hu, Z.H., Xiao, W., 2024. Low carbon dioxide emissions from aquaculture farm of lake revealed by long-term measurements. Agr Ecosyst Environ 363, 108851. https://doi.org/10.1016/j.agee.2023.108851.

Xu, H., Paerl, H.W., Qin, B.Q., Zhu, G.W., Gao, G., 2010. Nitrogen and phosphorus inputs control phytoplankton growth in eutrophic lake Taihu. China. Limnol. Oceanogr. 55, 420–432.

Yang, P., Lai, D.Y.F., Huang, J.F., Tong, C., 2018. Effect of drainage on CO_2, CH_4, and N_2O fluxes from aquaculture ponds during winter in a subtropical estuary of China. J. Environ. Sci. 65, 72–82. https://doi.org/10.1016/j.jes.2017.03.024.

Yang, P., Zhang, Y., Yang, H., Zhang, Y.F., Xu, J., Tan, L., Tong, C., Lai, D.Y., 2019. Large fine-scale spatiotemporal variations of CH_4 diffusive fluxes from shrimp aquaculture ponds affected by organic matter supply and aeration in Southeast China. J Geophys Res-Biogeo 124 (5), 1290–1307. https://doi.org/10.1029/2019JG005025.

Yang, P., Zhang, Y.F., Yang, H., Guo, Q.Q., Lai, D.Y.F., Zhao, G.H., Li, L., Tong, C., 2020. Ebullition was a major pathway of methane emissions from the aquaculture ponds in southeast China. Water Res. 184, 116176. https://doi.org/10.1016/j.watres.2020.116176.

Yang, P., Lai, D.Y.F., Yang, H., Lin, Y.X., Tong, C., Hong, Y., Tian, Y.L., Tang, C., Tang, K. W., 2022. Large increase in CH4 emission following conversion of coastal marsh to aquaculture ponds caused by changing gas transport pathways. Water Res. 222, 118882. https://doi.org/10.1016/j.watres.2022.118882.

Yang, P., Tang, K.W., Yang, H., Tong, C., Zhang, L.H., Lai, D.Y.F., Hong, Y., Tan, L.S., Zhu, W.Y., Tang, C., 2023. Contrasting effects of aeration on methane (CH_4) and nitrous oxide (N_2O) emissions from subtropical aquaculture ponds and implications for global warming mitigation. J. Hydrol. 617, 128876. https://doi.org/10.1016/j.jhydrol.2022.128876.

Yang, P., Su, Z.N., Tang, K.W., Yang, H., Tang, L.L., Zhang, L.H., Luo, J.H., Huang, J.F., Hu, M.J., Sun, D.Y., Qiu, G.L., 2024a. Plastic liners as a simple and effective approach to reduce CH_4 and N_2O emissions from aquaculture ponds. Agr Ecosyst Environ 375, 109191. https://doi.org/10.1016/j.agee.2024.109191.

Yang, P., Zhang, L.H., Lin, Y.X., Yang, H., Lai, D.Y., Tong, C., Zhang, Y.F., Tan, L.X., Zhao, G.H., Tang, K.W., 2024b. Significant inter-annual fluctuation in CO_2 and CH_4 diffusive fluxes from subtropical aquaculture ponds: Implications for climate change and carbon emission evaluations. Water Res. 249, 120943. https://doi.org/10.1016/j.watres.2023.120943.

Yuan, J.J., Xiang, J., Liu, D.Y., Kang, H., He, T.H., Kim, S., Lin, Y.X., Freeman, C., Ding, W.X., 2019. Rapid growth in greenhouse gas emissions from the adoption of industrial-scale aquaculture. Nat. Clim. Chang. 9 (4), 318–322. https://doi.org/10.1038/s41558-019-0425-9.

Yuan, J.J., Liu, D.Y., Xiang, J., He, T.H., Kang, H., Ding, W.X., 2021. Methane and nitrous oxide have separated production zones and distinct emission pathways in freshwater aquaculture ponds. Water Res. 190, 116739. https://doi.org/10.1016/j.watres.2020.116739.

Yvon-Durocher, G., Allen, A.P., Bastviken, D., Conrad, R., Gudasz, C., St-Pierre, A., Duc-Thanh, N., Del Giorgio, P.A., 2014. Methane fluxes show consistent temperature dependence across microbial to ecosystem scales. Nature 507 (7493), 488–491. https://doi.org/10.1038/nature13164.

Zhang, Y.L., Liu, X.H., Qin, B.Q., Shi, K., Deng, J.M., Zhou, Y.Q., 2016. Aquatic vegetation in response to increased eutrophication and degraded light climate in Eastern Lake Taihu: Implications for lake ecological restoration. Sci Rep 6, 23867. https://doi.org/10.1038/srep23867.

Zhang, C., Cheng, S.G., Li, Y.Z., Zhang, W.L., Xiao, S.B., 2019a. Diel methane flux from a subtropical eutrophic pond in November based on continuous monitoring. Acta Geochim 38, 232–240. https://doi.org/10.1007/s11631-019-00317-1.

Zhang, M., Xiao, Q.T., Zhang, Z., Gao, Y.Q., Zhao, J.Y., Pu, Y.N., Wang, W., Xiao, W., Liu, S.D., Lee, X.H., 2019. Methane flux dynamics in a submerged aquatic vegetation zone in a subtropical lake. Sci. Total Environ. 672, 400–409. https://doi.org/10.1016/j.scitotenv.2019.03.466.

Zhao, J.Y., Zhang, M., Xiao, W., Wang, W., Zhang, Z., Yu, Z., Xiao, Q.T., Cao, Z.D., Xu, J. Z., Zhang, X.F., Liu, S.D., Lee, X.H., 2019. An evaluation of the flux-gradient and eddy covariance method to measure CH_4, CO_2, and H_2O fluxes from small ponds. Agr Forest Meteorol 275, 255–264. https://doi.org/10.1016/j.agrformet.2019.05.032.

Zhao, J.Y., Zhang, M., Xiao, W., Jia, L., Zhang, X.F., Wang, J., Zhang, Z., Xie, Y.H., Pu, Y. N., Liu, S.D., Feng, Z.Z., Lee, X.H., 2021. Large methane emission from freshwater aquaculture ponds revealed by long-term eddy covariance observation. Agr Forest Meteorol 308, 108600. https://doi.org/10.1016/j.agrformet.2021.108600.

Zhang, D.X., He, J., Xu, W.J., Li, S., Liu, H.L., Chai, X.R., 2022a. Carbon dioxide and methane fluxes from mariculture ponds: The potential of sediment improvers to reduce carbon emissions. Sci. Total Environ. 829, 154610. https://doi.org/10.1016/j.scitotenv.2022.154610.

Zhang, W.B., Belton, B., Edwards, P., Henriksson, P.J.G., Little, D.C., Newton, R., Troell, M., 2022b. Aquaculture will continue to depend more on land than sea [J]. Nature 603 (7900), E2–E4. https://doi.org/10.1038/s41586-021-04331-3.

Zhang, Y.P., Qin, Z.C., Li, T.T., Zhu, X.D., 2022c. Carbon dioxide uptake overrides methane emission at the air-water interface of algae-shellfish mariculture ponds: Evidence from eddy covariance observations. Sci. Total Environ. 815, 152867. https://doi.org/10.1016/j.scitotenv.2021.152867.

Zhang, Y.F., Tang, K.W., Yang, P., Yang, H., Tong, C., Song, C.C., Tan, L.S., Zhao, G.H., Zhou, X.D., Sun, D.Y., 2022d. Assessing carbon greenhouse gas emissions from aquaculture in China based on aquaculture system types, species, environmental conditions and management practices. Agr Ecosyst Environ. 338, 108110. https://doi.org/10.1016/j.agee.2022.108110.

Zhang, L.Q., Xu, Y.J., Ma, B.J., Jiang, P., Li, S.Y., 2023a. Intense methane diffusive emissions in eutrophic urban lakes. Central China. Environ Res. 237, 117073. https://doi.org/10.1016/j.envres.2023.117073.

Zhang, Y.P., Guo, X.H., Zhu, X.D., 2023b. Strong diurnal variability of carbon dioxide flux over algae-shellfish aquaculture ponds revealed by eddy covariance measurements. Agr Ecosyst Environ. 348, 108426. https://doi.org/10.1016/j.agee.2023.108426.

Zhang, L.L., Wang, X.H., Huang, L., Wang, C.Z., Gao, Y.Y., Peng, S.S., Canadell, J., Piao, S.L., 2024. Inventory of methane and nitrous oxide emissions from freshwater aquaculture in China. Commun Earth Environ. 5, 531. https://doi.org/10.1038/s43247-024-01699-8.

Zhou, Y.W., Song, K., Han, R.M., Riya, S.H., Xu, X.G., Yeerken, S., Geng, S.X., Ma, Y., Terada, A., 2020. Nonlinear response of methane release to increased trophic state levels coupled with microbial processes in shallow lakes. Environ Pollut 265, 114919. https://doi.org/10.1016/j.envpol.2020.114919.

Zhu, D., Wu, Y., Chen, H., He, Y.X., Wu, N., 2016. Intense methane ebullition from open water area of a shallow peatland lake on the eastern Tibetan Plateau. Sci. Total Environ. 542, 57–64. https://doi.org/10.1016/j.scitotenv.2015.10.087.

Zhu, Y.Z., Purdy, K.J., Eyice, Ö., Shen, L.D., Harpenslager, S.F., Yvon-Durocher, G., Dumbrell, A.J., Trimmer, M., 2020. Disproportionate increase in freshwater methane emissions induced by experimental warming. Nat. Clim. Chang. 10, 685–690. https://doi.org/10.1038/s41558-020-0824-y.

Znachor, P., Nedoma, J., Kolar, V., Matoušů, A., 2023. Spatial and temporal variability of methane emissions and environmental conditions in a hyper-eutrophic fishpond. Biogeosciences 20 (20), 4273–4288. https://doi.org/10.5194/bg-20-4273-2023.